

# Vehicles dynamics, planning and control of robotic cars.

Rajat Sahore, UNITN, rajat.sahore@studenti.unitn.it

## Assignments Report - 2021

The EIT Digital – European entrepreneurs driving digital innovation & education

EIT Digital

Rajat Sahore / February 2020

[www.eitdigital.eu](http://www.eitdigital.eu)

Table of contents:

<b>1. Assignment 1 .....</b>	<b>3</b>
1.1 Exercise 1: - Pure longitudinal slip .....	3
o Exercise 1.1: - Pure longitudinal force .....	3
o Exercise 1.2: - Computing longitudinal slip.....	3
o Exercise 1.3: - Computation of longitudinal stiffness .....	4
1.2 Exercise 2: - Combined slip .....	4
o Exercise 2.1: - Side slip angle & combined tire force.....	4
o Exercise 2.2: - Combined longitudinal tire force .....	4
<b>2. Assignment 2 .....</b>	<b>5</b>
2.1 Exercise 1: - Understanding tire data .....	5
o Exercise 1.1: - Raw data plot .....	5
o Exercise 1.2: - $F_x$ vs $\kappa$ for $\alpha = 0$ and $\gamma = 0$ .....	6
o Exercise 1.3: - $F_x$ vs $\kappa$ for $F_z = 670N$ and $\gamma = 0$ .....	7
2.2 Exercise 2: - Fitting tire data .....	7
o Exercise 2.1: - Fit the coefficients $X_1$ .....	7
o Exercise 2.2: - Fit the coefficients $X_2$ .....	8
o Exercise 2.3: - Fit the coefficients $X_3$ .....	8
<b>3. Assignment 3 .....</b>	<b>9</b>
3.1 Exercise 1: - Vehicle model implementation .....	9
o Exercise 1.1: - Maneuver 1 Simulation .....	9
o Exercise 1.2: - Maneuver 2 Simulation .....	12
o Exercise 1.3: - Maneuver 3 Simulation .....	13
<b>4. Assignment 4 .....</b>	<b>16</b>
4.1 Exercise 1: - Sine steer maneuvers .....	16
o Exercise 1.1: - Sine steer maneuver 1.....	16
o Exercise 1.2: - Sine steer maneuver 2.....	17
o Exercise 1.3: - Sine steer maneuver 3.....	19
4.2 Exercise 1.2: - Sine steer maneuvers .....	20
o Exercise 1.1: - Sine steer maneuver 1.....	20
o Exercise 1.1: - Sine steer maneuver 2.....	22

o	Exercise 1.1: - Sine steer maneuver 3.....	23
4.3	Exercise 2: - Constant steer maneuvers .....	25
o	Exercise 2.1: - Constant steer maneuver 1 .....	25
o	Exercise 2.2: - Constant steer maneuver 2 .....	26
o	Exercise 2.3: - Pros and Cons .....	28
<b>5.</b>	<b>Assignment 5 .....</b>	<b>28</b>
5.1	Exercise 1: - Lateral Control.....	28
o	Exercise 1.1: - Clothoid-based lateral controller .....	28
o	Exercise 1.2: - Pure pursuit controller .....	30
o	Exercise 1.3: - Stanley kinematic controllers .....	32
o	Exercise 1.4: - Stanley dynamic controllers .....	34
o	Exercise 1.5: - Pros and cons .....	36
<b>6.</b>	<b>Assignment 6 .....</b>	<b>37</b>
6.1	Exercise 1: - Route planning .....	37
o	Exercise 1.1: - Optimizing RRT* .....	37
o	Exercise 1.2: - Clothoid fitting vs dubins paths .....	40
o	Exercise 1.2: - Efficiency of RRT* for route planning and the limitations .....	40
6.2	Exercise 2: - Lateral Control.....	41
o	Exercise 2.1: - Clothoids Controller .....	41
o	Exercise 2.2: - Pure pursuit controller .....	43
o	Exercise 2.3: - Stanley kinematic controllers .....	45
o	Exercise 2.4: - Stanley dynamic controllers .....	48

# 1. Assignment 1

## 1.1 Exercise 1: - Pure longitudinal slip

- **Exercise 1.1: - Pure longitudinal force**

In this exercise, I used the parameters given in the assignment and used the Pacejka Magic Formula to obtain a plot the longitudinal tire force  $F_{x0}$  in pure longitudinal slip conditions, as a function of slip. The plot is shown in Fig. 1.

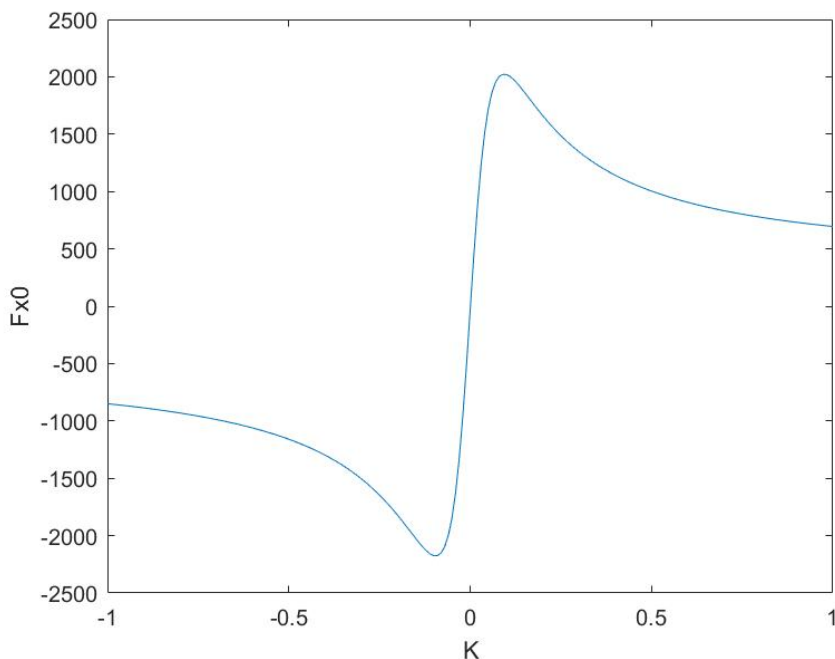


Fig. 1 Plot of pure longitudinal force ( $F_{x0}$ ) vs slip ( $\kappa$ )

From this graph we can see that with the increase in the value of longitudinal slip, the value of  $F_{x0}$  also increases until reaching a saturation limit that depends upon the Vertical load ( $F_{x0}$ ).

If I were supposed to design a traction control system for maximizing the vehicle's longitudinal acceleration, the target value of longitudinal slip ( $\kappa$ ) would be 0.1 that gives the maximum force value of  $F_{x0} = 2022$  N.

- **Exercise 1.2: - Computing longitudinal slip.**

In the given conditions in the assignment, the value of longitudinal slip ( $\kappa$ ) 0.0769. In this condition the tire is accelerating as the value of longitudinal slip ( $\kappa$ )  $> 0$ . The corresponding longitudinal tire force  $F_{x0}$  is 1990.7 N.

- **Exercise 1.3: - Computation of longitudinal stiffness**

The longitudinal stiffness  $C_{fk}$  that is the derivative of the  $F_{x0}$  function at  $\kappa = 0$  is 472.2186. For the values of  $\kappa$  in between the range [-0.1,0.1] gives the linear approximation of Pacejka curve. This can be seen in Fig. 1.

## 1.2 Exercise 2: - Combined slip

- **Exercise 2.1: - Side slip angle & combined tire force**

The side slip angle  $\alpha = 0.0865$ .

The combined tire force  $F_x = 1448.3$ .

- **Exercise 2.2: - Combined longitudinal tire force**

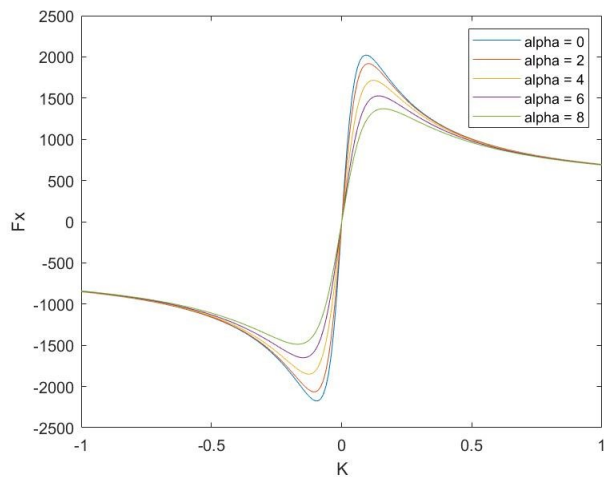


Fig. 2 Plot of combined longitudinal force ( $F_x$ ) vs slip ( $\kappa$ )

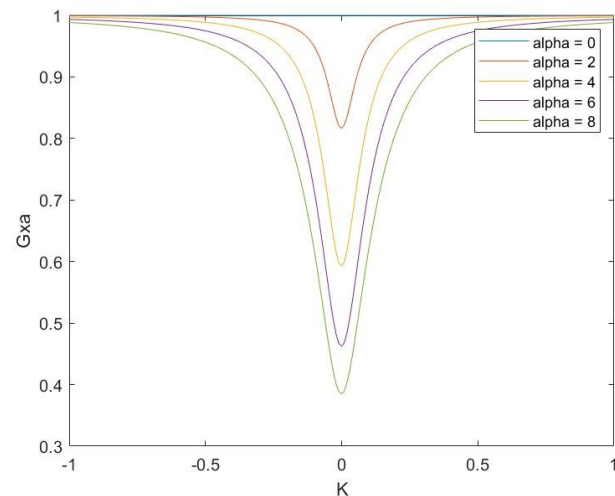


Fig. 3 Plot of Weighting function ( $G_{xa}$ ) vs slip ( $\kappa$ )

The plot of combined longitudinal force ( $F_x$ ) vs slip ( $\kappa$ ) is shown in Fig. 2 and the plot of Weighting function ( $G_{xa}$ ) vs slip ( $\kappa$ ) is shown in Fig. 3. From Fig. 2 we can infer that the peak value of combined longitudinal force ( $F_x$ ) is reduced with increase in the side slip angle  $\alpha$  from 0 to 8 degrees. This is because combined longitudinal force ( $F_x$ ) depends on weighting function ( $G_{xa}$ ) as given in the equation below:

$$F_x = G_{xa} F_{x0}$$

The weighting function ( $G_{xa}$ ) is calculated as given in the equation below:

$$G_{xa} = D_{xa} \cos (C_{xa} \arctan (B_{xa} (\alpha + S_{Hxa})))$$

It is clear from this equation that with increase in the side slip angle  $\alpha$ , the value of arctan value will increase and the value of cos function will reduce. Ultimately, the value of  $G_{xa}$  and  $F_x$  will also be reduced. Also, due to change  $G_{xa}$  the value of the cornering stiffness changes which is  $B*C*D$  in the resulting  $F_x$  as we increase the side slip angle  $\alpha$ .

## 2. Assignment 2

### 2.1 Exercise 1: - Understanding tire data.

- Exercise 1.1: - Raw data plot

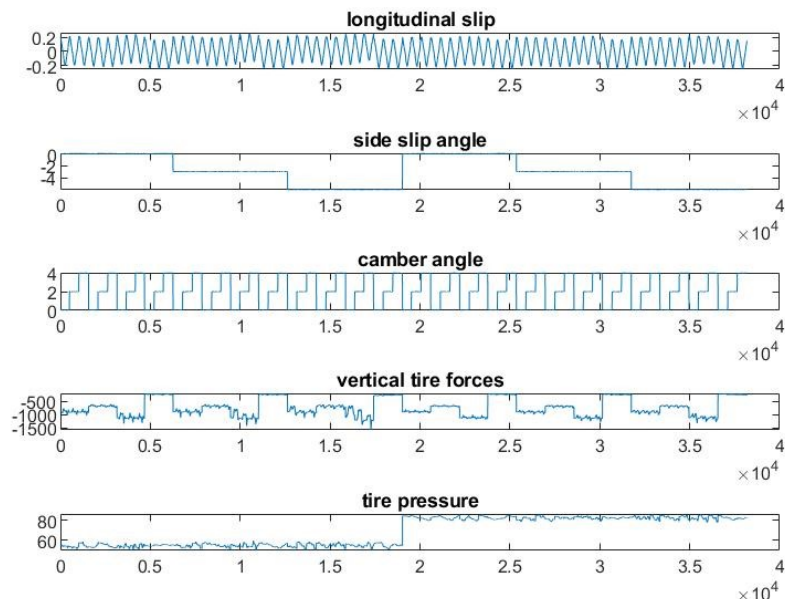


Fig. 4 Raw data plot

In the Fig. 4, we can see that the tests are carried out in with four different values of the vertical loads  $F_Z$  i.e. (1100, 900, 690, 230) (approx.), three different values of the side slip angle i.e. (0, 3, 6) degrees, two tire pressure values i.e. (82, 52) kPa (approx.) and three different values of the camber angle i.e. (0, 2, 4) degrees. We can observe that in the Fig. 4 is the longitudinal slip and the camber angle parameters changes frequently. This tire data can be used to fit in the Pacejka Magic Formula to compute the various coefficients and make a fitting curve. The curves can then be used to accurately predict tire performance in the various operating conditions.

- **Exercise 1.2: -  $F_x$  vs  $\kappa$  for  $\alpha = 0$  and  $\gamma = 0$**

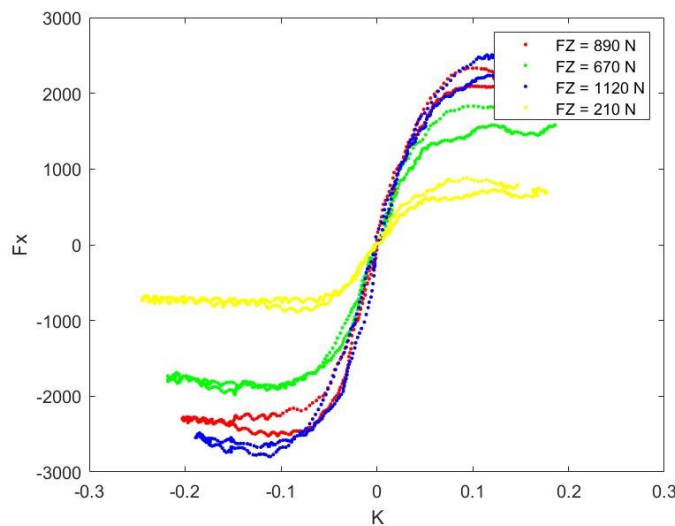


Fig. 5 Longitudinal Force  $F_x$  vs slip ( $\kappa$ ) for  $\alpha = 0$  and  $\gamma = 0$

Observing the Fig. 5, the Longitudinal Force ( $F_x$ ) increases with the increase in the value of vertical load ( $F_z$ ). With increase in the slip angle ( $\kappa$ ) the Longitudinal Force ( $F_x$ ) the curve is nonlinear, and the Longitudinal Force ( $F_x$ ) saturates after a certain value when seen with respect to variation in slip angle ( $\kappa$ ). This data is analyzed at the lower pressure value i.e., 52 kPa (approx.).

- Exercise 1.3: -  $F_x$  vs  $\kappa$  for  $F_z = 670N$  and  $\gamma = 0$

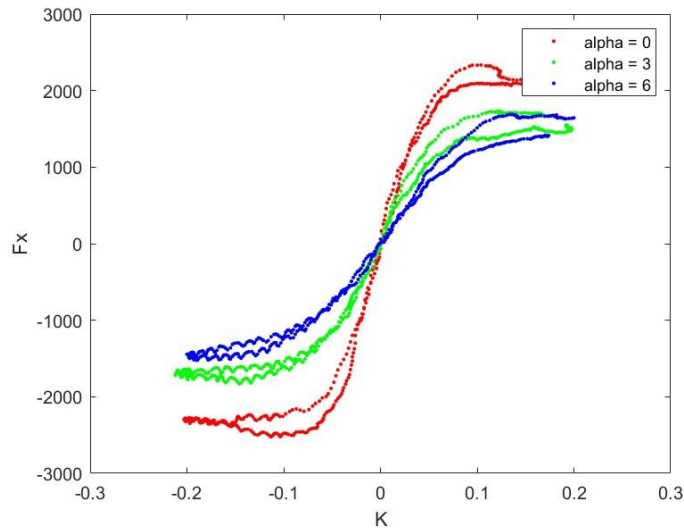


Fig. 6 Longitudinal Force  $F_x$  vs slip ( $\kappa$ ) for  $F_z = 670N$  and  $\gamma = 0$

Observing the Fig. 6, Longitudinal Force  $F_x$  value decreases with the increase in the side slip angle. This is due to the reason discussed in Ex 2.2 of Assignment 1. Hence, a reduction in the peak of the curve is observed. Also, the cornering stiffness value is changed as explained in Ex 2.2 of Assignment 1. This data is analyzed at the lower pressure value i.e., 52 kPa (approx.).

## 2.2 Exercise 2: - Fitting tire data

- Exercise 2.1: - Fit the coefficients  $X_1$ .

Conditions:  $F_{z0} = 890$ ,  $\alpha = 0$ ,  $\gamma = 0$  and pressure = 82 kPa

Compute  $X_1 = p_{Cx1}, p_{Dx1}, p_{Ex1}, p_{Ex4}, p_{Kx1}, p_{Hx1}, p_{Vx1}$

As shown in Fig.7 we can clearly see that the curve is well fitted. With increase in the value of longitudinal force the fitted curve almost follows the raw data and with increase in the value of slip ( $\kappa$ ), the longitudinal force also increases.

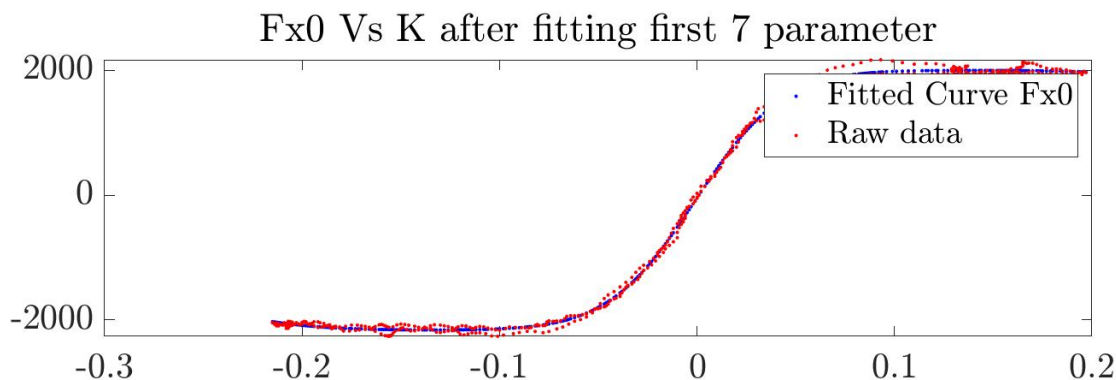


Fig. 7 Longitudinal Force  $F_x$  vs slip ( $\kappa$ ) after first fitting

- **Exercise 2.2: - Fit the coefficients  $X_2$ .**

Conditions:  $F_{z0} =$  four different values (1100, 900, 690, 230) (approx.),  $\alpha = 0$ ,  $\gamma = 0$  and pressure = 82kPa

Compute  $X_2 = p_{Dx2}, p_{Ex2}, p_{Ex3}, p_{Hx2}, p_{Kx2}, p_{Vx2}$

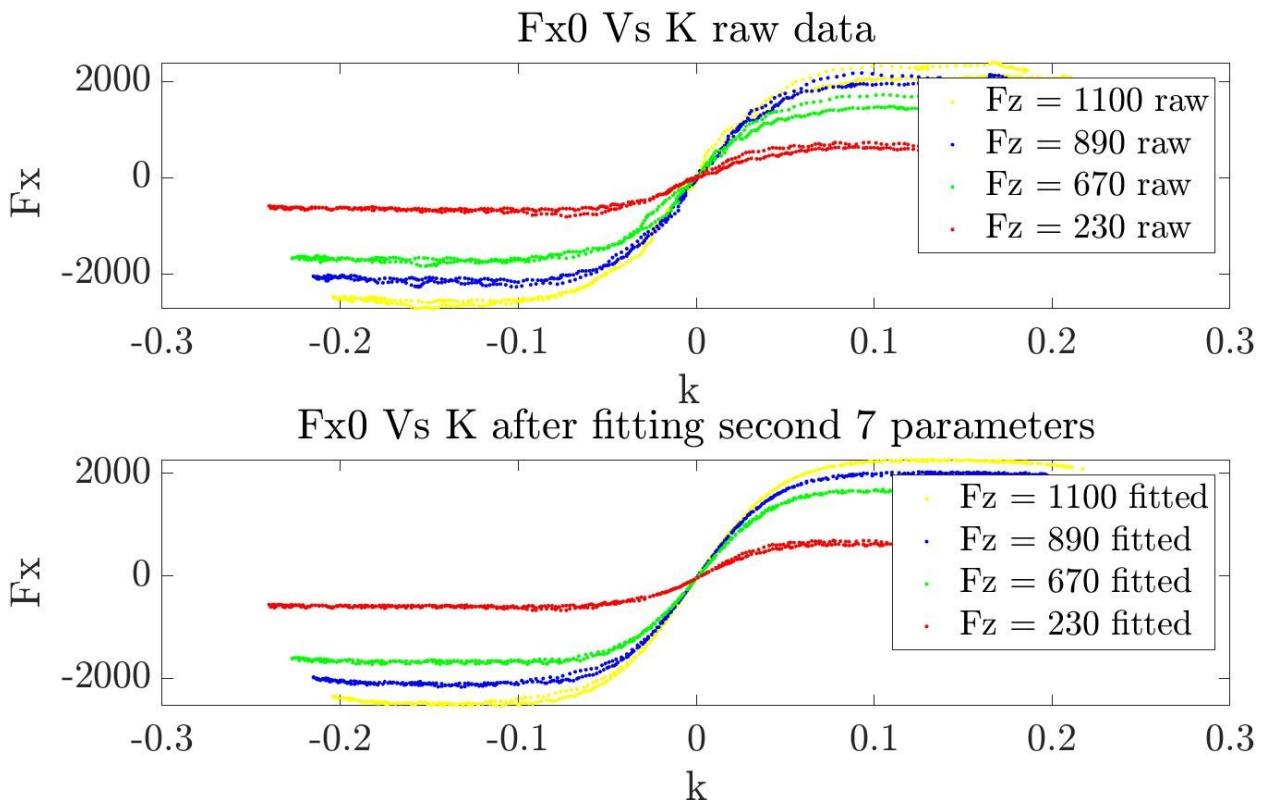


Fig. 8 Longitudinal Force  $F_x$  vs slip ( $k$ ) after second fitting

As shown in Fig. 8, the fitted curve matches with the raw data, the Longitudinal Force  $F_x$  reaches a saturation above a certain level of the slip ( $k$ ). Note that the longitudinal stiffness at vertical load  $F_z = 230$  is not high as seen for the other values of vertical load  $F_z$ .

- **Exercise 2.3: - Fit the coefficients  $X_3$ .**

Conditions:  $F_{z0} = 890$ ,  $\alpha = 0$ ,  $\gamma =$  three different values and pressure = 82kPa

Compute  $X_3 = p_{Dx3}$

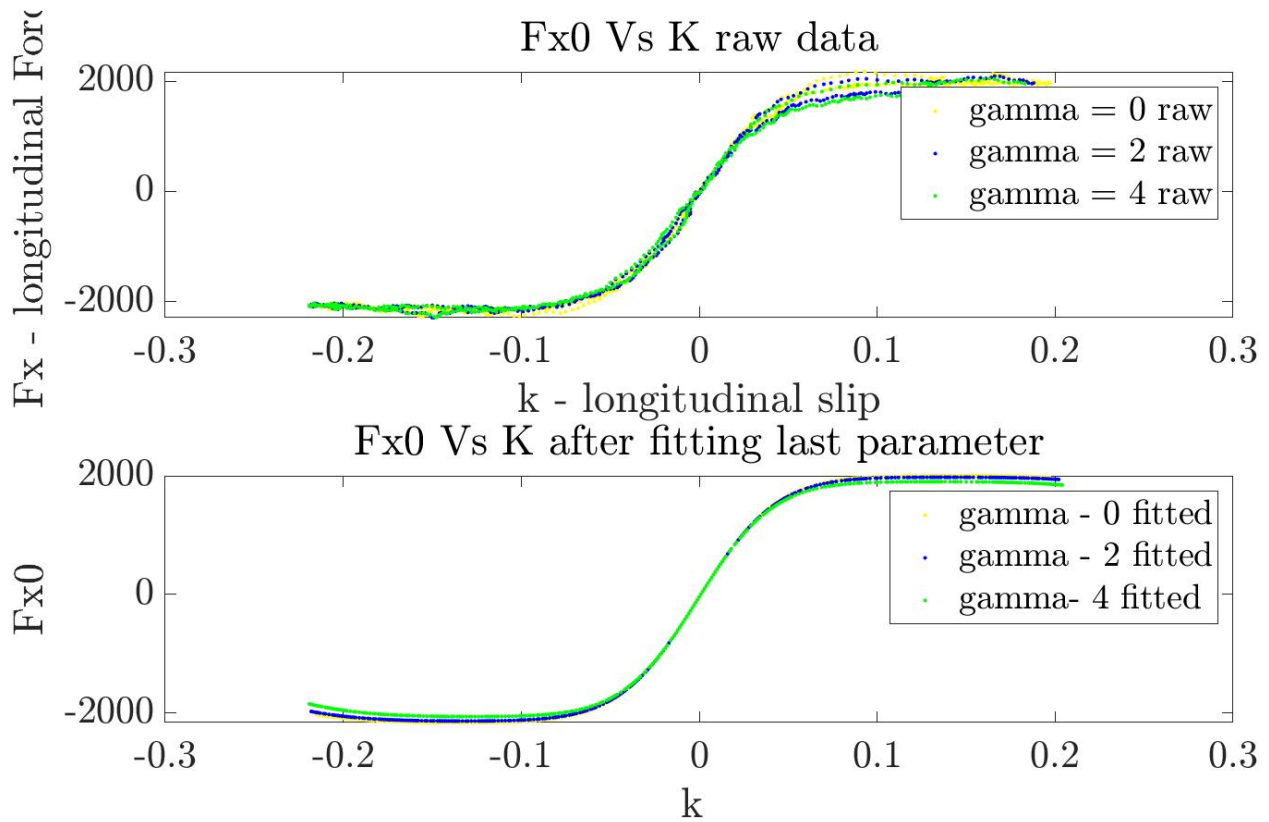


Fig. 9 Longitudinal Force  $F_x$  vs slip ( $\kappa$ ) after final fitting

As shown in Fig. 9, the fitted curve resembles completely and is very close with the raw data values in terms of longitudinal, stiffness and saturation. With the increase in the camber values, the longitudinal force peak values also reduce as seen in the raw data as well. The final value of all the computed coefficients of the Pacejka Magic Formula is given below:

$$X = [2.5974, 2.3458, -0.6628, 9.7963, 1.6904, 0.5695, 0.1949, 0.0255, 53.4591, 0.0901, 0.6294, 0.0009, 0.0055, -0.0954, -0.1806]$$

### 3. Assignment 3

#### 3.1 Exercise 1: - Vehicle model implementation

- [Exercise 1.1: - Maneuver 1 Simulation](#)

Conditions: initial conditions:  $u_0 = 30 \text{ km/h}$  simulation timing:  $T_s = 0:001 \text{ s}$ ,  $T_f = 20 \text{ s}$

requested pedal: req pedal = 1 requested steering wheel angle: req steer = 0 deg.

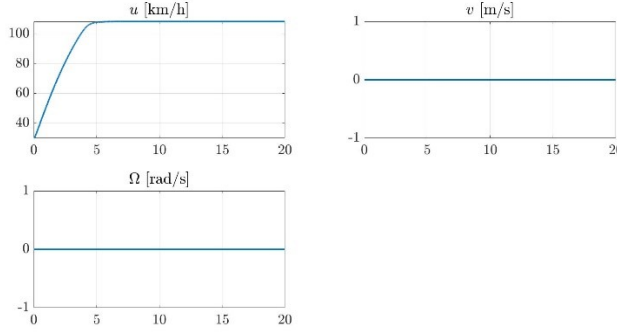


Fig. 10 Velocity profile for the Maneuver 1

As per the given conditions, the vehicle accelerates in the straight motion due to full throttle and zero steer. This is clearly depicted in Fig. 10. We can also observe from the graph that the car can reach to a maximum velocity limit of 120 Km/hr.

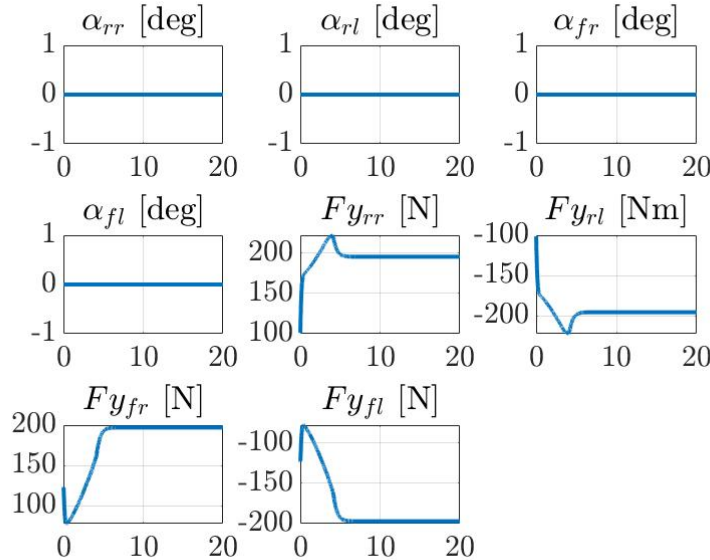


Fig. 11 Lateral forces & side slip angle ( $\alpha$ )

As shown in Fig. 11 the lateral slip value is zero because the requested steering angle is zero in the conditions. The tire forces are calculated with the help of pacjeka model so the lateral force is dependent on vertical load, camber, and the longitudinal slip. The lateral force value is small compared to the longitudinal and vertical forces at the contact point in the given conditions.

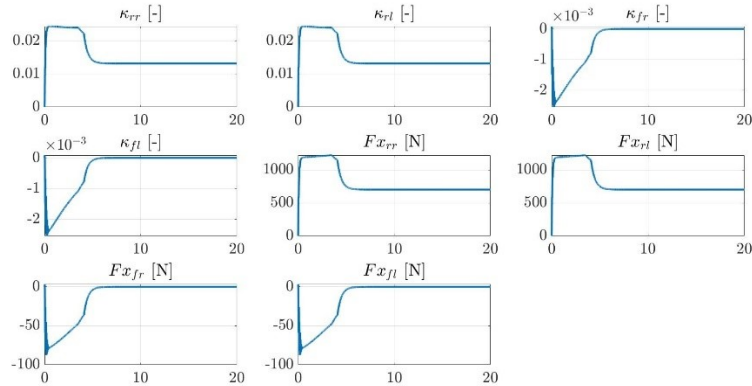


Fig. 12 Longitudinal forces & slip ( $\kappa$ )

As shown in the figure 12, the longitudinal slip ( $\kappa$ ) value and longitudinal forces are different for each tire because the rotational speed is different for each tire. We can clearly observe from the graphs that both the values are more for the rear tires compared to the front tires. This is because the wheel torque is addition of motor and brake torques but for the rear tires also have the effect of traction torques added from the motor model which results in more slip and force on the rear wheels.

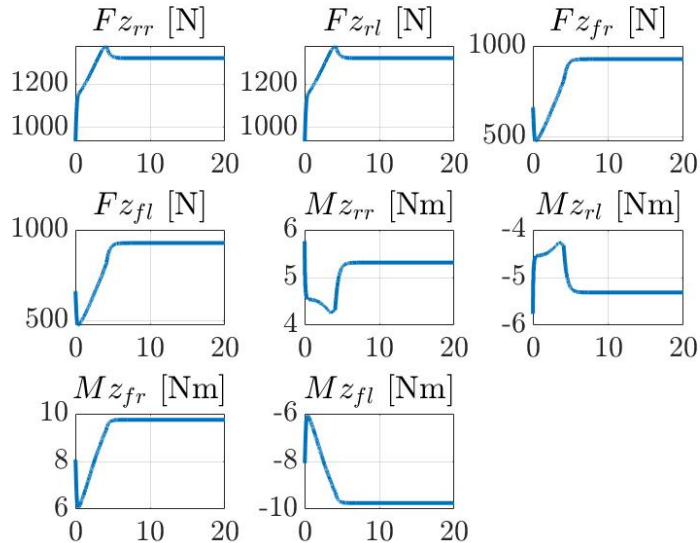


Fig. 13 Vertical forces and self-aligning torque

As shown in the figure 13, the vertical forces for the rear tires are more than the front tires because the force values depend upon, the aerodynamic forces and drag. The self-aligning torque values are different for each tire to counter the lateral forces. The vehicle is in accelerating condition, so the effect of lateral forces is positive on the self-aligning torque values.

- **Exercise 1.2: - Maneuver 2 Simulation**

Conditions: initial conditions:  $u_0 = 100 \text{ km/h}$  simulation timing:  $T_s = 0:001 \text{ s}$ ,  $T_f = 1.5 \text{ s}$

requested pedal: req pedal = -1 requested steering wheel angle: req steer = 0 deg.

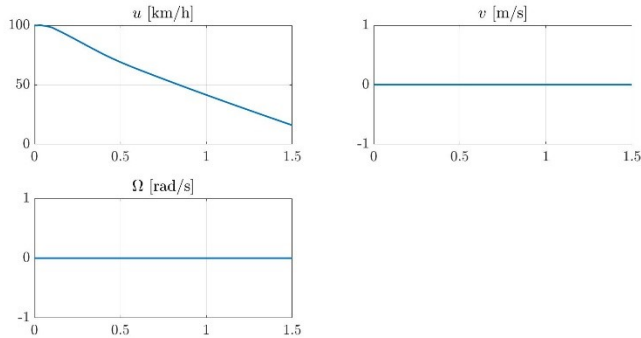


Fig. 14 Velocity profile for the Maneuver 2

As per the given conditions, the vehicle decelerates in the straight motion due to full throttle and zero steer. This is clearly depicted in Fig. 14. We can also observe from the graph that the car cannot come to a full stop in simulation time of 1.5 sec, it needs more time for stopping from the speed of 100 Km/hr to 0 Km/hr.

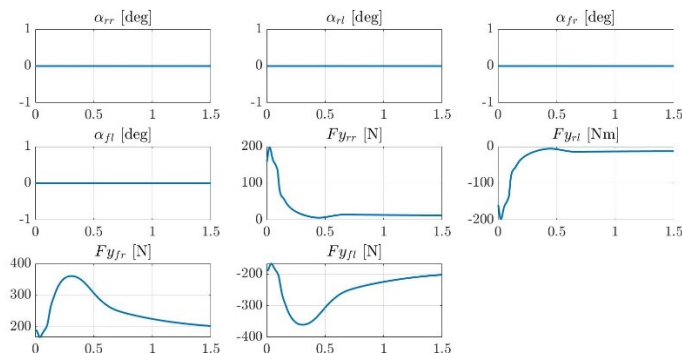


Fig. 15 Lateral forces & side slip angle ( $\alpha$ )

As shown in Fig. 15 the lateral slip value is zero because the requested steering angle is zero in the conditions. The tire forces are calculated with the help of pacjeka model so the lateral force is dependent on vertical load, camber, and the longitudinal slip. We can observe from the graphs that the lateral forces are same for front tires, and for the rear tires in the braking condition at the contact point. This can be due to the dependence of lateral forces on the parameters such as vertical load, camber, and the longitudinal slip which we will investigate in the next figures.

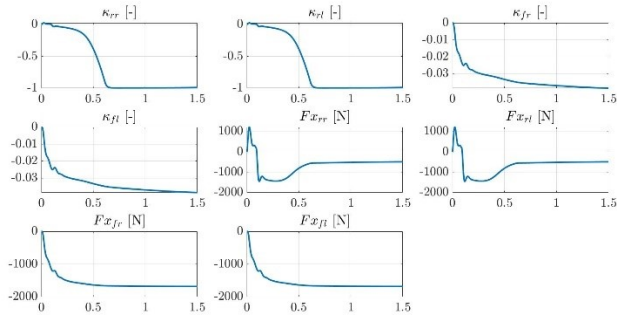


Fig. 16 Longitudinal forces & slip ( $\kappa$ )

As shown in Fig. 16, the Longitudinal forces slip ( $\kappa$ ) is same for the front tires and for the rear tires. We also observe from the graph that the rear wheels go in the locking conditions fast after 0.5 sec i.e.,  $\kappa = -1$ . All the tires have a negative slips value due to braking condition to stop the vehicle.

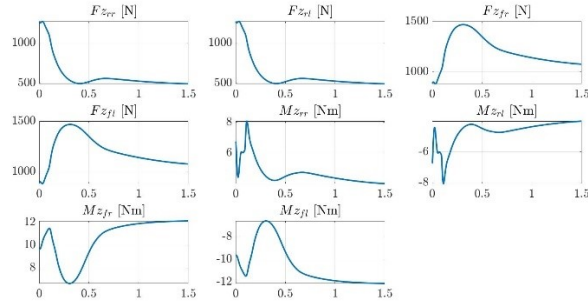


Fig. 17 Vertical forces and self-aligning torque

As shown in Fig. 17, the vertical force on front tires is more than the rear tires. This is due to the braking condition and the aerodynamic down forces and drag. The value is same for both front tires and same case for the rear tires as well. The self-aligning torque values show the same trend as the vertical force for the front and rear tires. The vehicle is in decelerating condition, so the effect of lateral forces is negative on the self-aligning torque values.

- **Exercise 1.3: - Maneuver 3 Simulation**

Conditions: initial conditions:  $u_0 = 50 \text{ km/h}$  simulation timing:  $T_s = 0:001 \text{ s}$ ,  $T_f = 10 \text{ s}$

requested pedal: req pedal = 0.5 requested steering wheel angle: req steer = 20 deg.

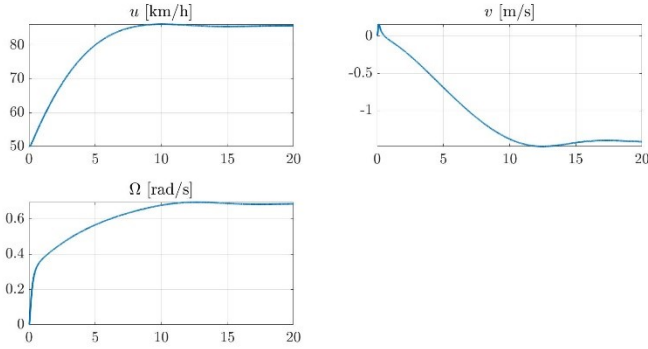


Fig. 18 Velocity profile for the Maneuver 3

As seen in Fig. 18, there is a constant increase in the longitudinal direction due to constant throttle pedal. The lateral forces are negative that suggests that the vehicle is steered to the left direction. We also observe the yaw rate of the vehicle, because of the turning condition. The value increases in the start and then become constant after longitudinal speed is constant.

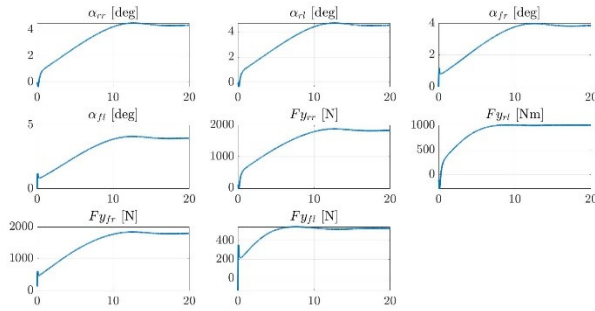


Fig. 19 Lateral forces & side slip angle ( $\alpha$ )

As seen in the Fig. 19, there is a side slip angle ( $\alpha$ ) due to the applied steering angle. As described in the double track lecture slides, the side slip angle is computed by the following equations:

$$\alpha_{fr} = - (v + (L_f \Omega) - \delta (u + W_f \Omega / 2)) / (u + (W_f \Omega / 2) + \delta (L_f \omega))$$

$$\alpha_{fl} = - (v + (L_f \Omega) - \delta (u - W_f \Omega / 2)) / (u - (W_f \Omega / 2) + \delta (L_f \omega))$$

$$\alpha_{rr} = - (v - (L_r \Omega)) / (u + (W_r \Omega / 2))$$

$$\alpha_{rl} = - (v - (L_r \Omega)) / (u - (W_r \Omega / 2))$$

Where,  $\Omega$  is the yaw rate of vehicle,  $u$  being the longitudinal velocity and  $v$  being lateral velocity of the vehicle.

From the graph we observe that the side slip angle ( $\alpha$ ) of all the tires is almost same. This is because  $u \gg (W_r \Omega / 2)$  and  $u \gg (W_f \Omega / 2)$ . We can also observe that the slip angles develop instantaneously for the front tires than the rear tires.

We can also observe that the lateral forces on all the tires are different, the force on the right tires are more than that of the left tires even though the slip value is almost similar. This is because the vehicle is taking a left turn, and the longitudinal slip and vertical load difference in the right and

the left tires. The lateral forces are developed immediately for the front tires than for the rear tires because the steering is applied on the front tires.

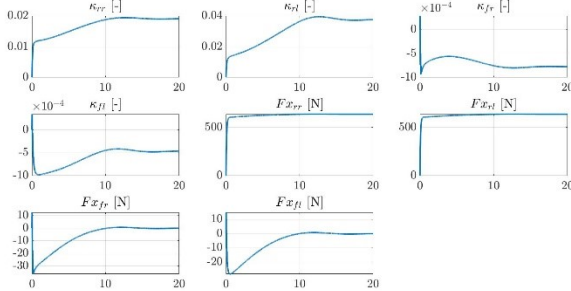


Fig. 20 Longitudinal forces & slip ( $\kappa$ )

As seen in the Fig. 20, there is a longitudinal slip angle ( $\kappa$ ) different in all the tires. As described in the double track lecture slides, longitudinal slip angle is computed by the following equations for  $u \gg (W_r \Omega / 2)$  and  $u \gg (W_f \Omega / 2)$ :

$$\kappa_{rr} = (\omega_{rr} R_r - u) / u$$

$$\kappa_{rl} = (\omega_{rl} R_r - u) / u$$

$$\kappa_{fr} = (\omega_{fr} R_f - u) / u$$

$$\kappa_{fl} = (\omega_{fl} R_f - u) / u$$

When turning the rotation speed of tires is different since both tires must cover different distances value when turning. So, the value of longitudinal slip angle ( $\kappa$ ) is different for each tire. Similarly, the longitudinal forces on the tires will also be different.

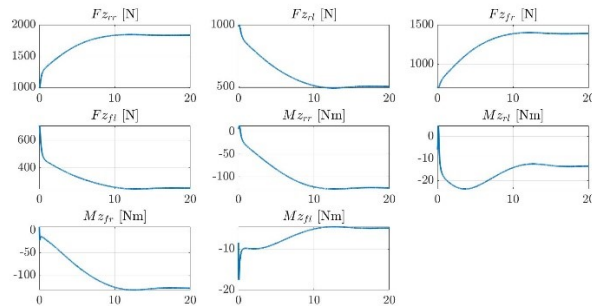


Fig. 21 Vertical forces and self-aligning torque

As shown in Fig. 21 the vertical load on the left tires is less than the right tires since we are steering left. The vehicle is accelerating so the force on rear wheels is more than the front wheels due to the aerodynamic forces and drag. The self-aligning torque is dependent on the lateral forces which is different for left and right tires in this case as the vehicle is turning. Hence the self-aligning torques are higher for left tires than the right tires. All the values of the self-aligning torque that means they oppose the lateral forces.

# 4. Assignment 4

## 4.1 Exercise 1: - Sine steer maneuvers

- **Exercise 1.1: - Sine steer maneuver 1**

Conditions:  $u=50\text{Km/h}$  and  $\delta_{D0} = 5^\circ$

I used the simulation run time of 1000 and frequency of 0.001Hz for this exercise. The handling diagram at this condition is depicted in Fig. 22.

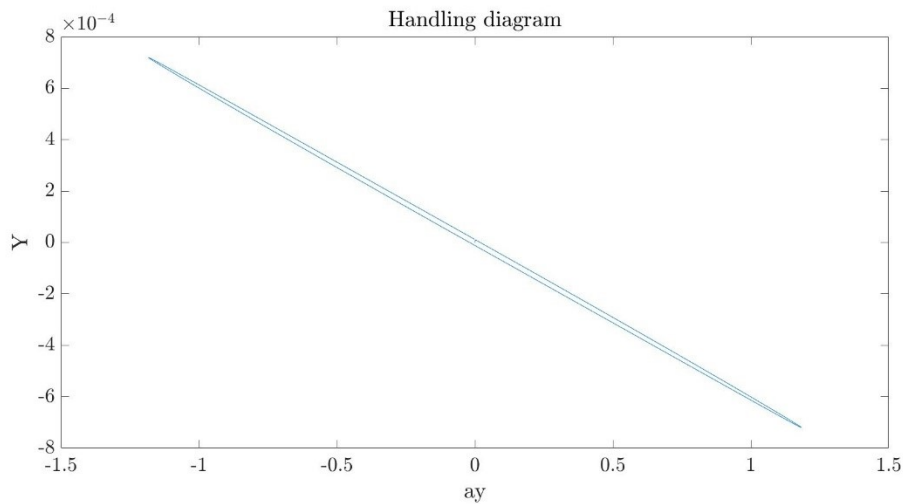


Fig. 22 Handling Diagram of maneuver 1

The curve is of the form of an ellipse downwards, so the vehicle has oversteer behaviors. Since  $a_y$  is small, the handling diagram can be approximated with a line.

$$Y = c_1 a_y + c_2$$

In this case,  $c_1 = -0.606940 \times 10^{-3}$  and  $c_2 = -0.000002 \times 10^{-3}$

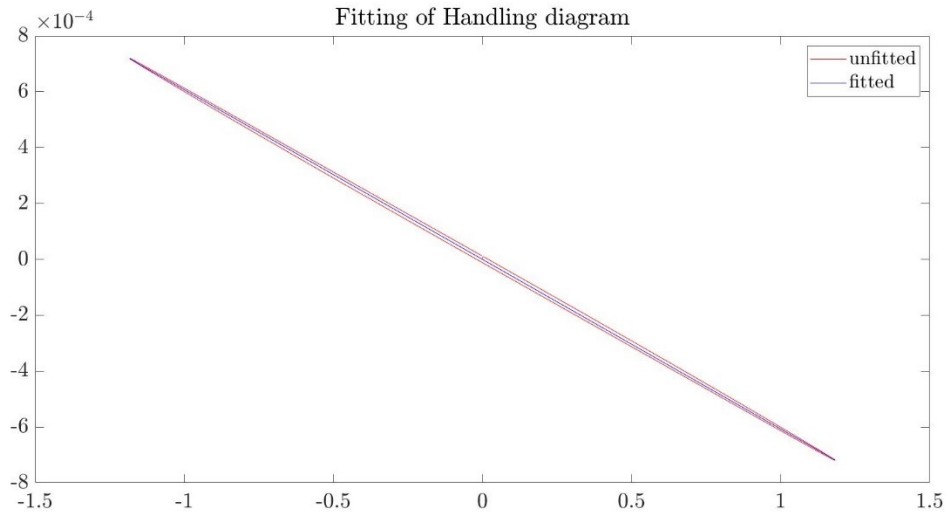


Fig. 23 Handling Diagram fitting of maneuver 1

The fitting curve is depicted in Fig. 23. From the fitted line we can depict that for left steer (positive  $a_y$ ), the vehicle is in oversteering condition. For right steer (negative  $a_y$ ), the vehicle is in understeering condition. The resulting curve of the handling diagram does not pass through the origin (when  $a_y = 0$  condition). The value of Y is very small because  $a_y$  and the coefficients are very small. Hence, the effect is not very much at lower speeds. It can be seen in Fig. 24.

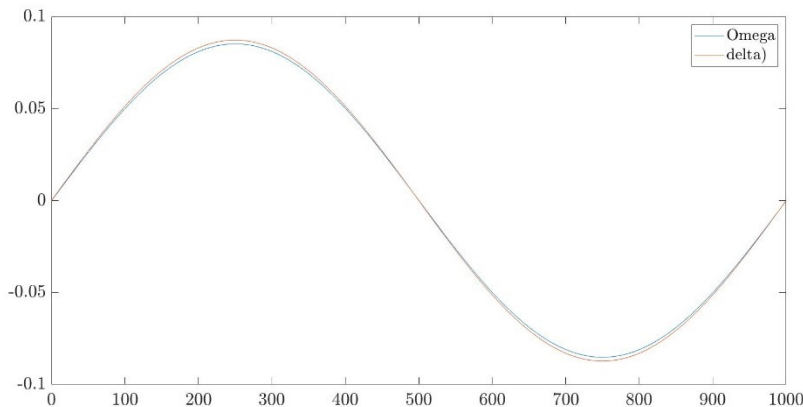


Fig. 24 Omega vs Delta for maneuver 1

- **Exercise 1.2: - Sine steer maneuver 2**

Conditions:  $u=80\text{Km/h}$  and  $\delta_{00} = 5^\circ$

I used the simulation run time of 1000 and frequency of 0.001Hz for this exercise. The handling diagram at this condition is depicted in Fig. 25.

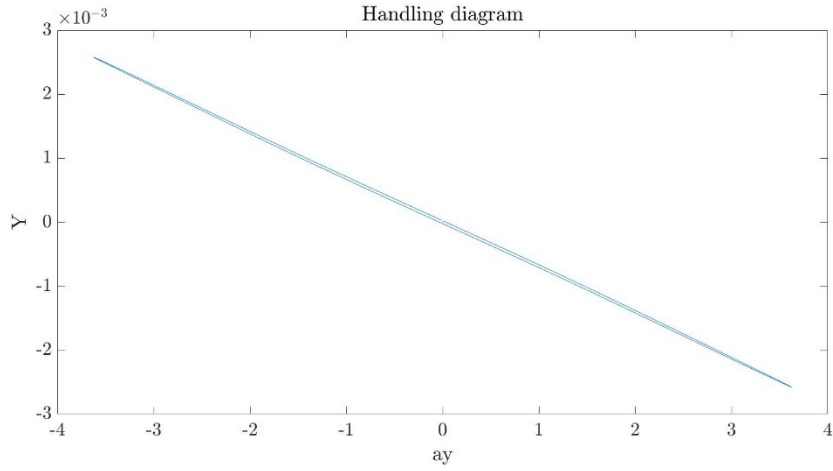


Fig. 25 Handling Diagram of maneuver 2

The curve is of the form of an ellipse going downwards, so the vehicle has oversteering behaviors as the previous case, but the value of handling behavior( $Y$ ) has increased from the previous case because speed and yaw rate are increased. It can also be observed from the coefficients value. Since  $a_y$  is small, the handling diagram can be approximated with a line.

$$Y = c_1 a_y + c_2$$

In this case,  $c_1 = -0.70850 \times 10^{-3}$  and  $c_2 = -0.000009 \times 10^{-3}$

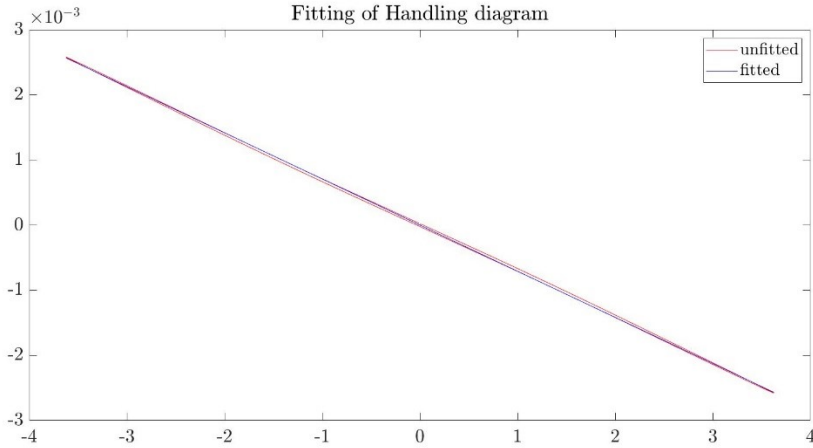


Fig. 26 Handling Diagram fitting of maneuver 2

The fitting curve is depicted in Fig. 26. From the fitted line we can depict that for left steer (positive  $a_y$ ), the vehicle is in oversteering condition. For right steer (negative  $a_y$ ), the vehicle is in oversteering condition. The resulting curve of the handling diagram does not pass through the origin (when  $a_y = 0$  condition). The value of  $Y$  has increased than the previous case because  $a_y$  and the coefficients have increased. Hence, the effect can be clearly observed now. It can be seen in Fig. 27. Through this curve we can observe that the vehicle did not follow the desired maneuver. There is a big oversteer when vehicle is turning left and right.

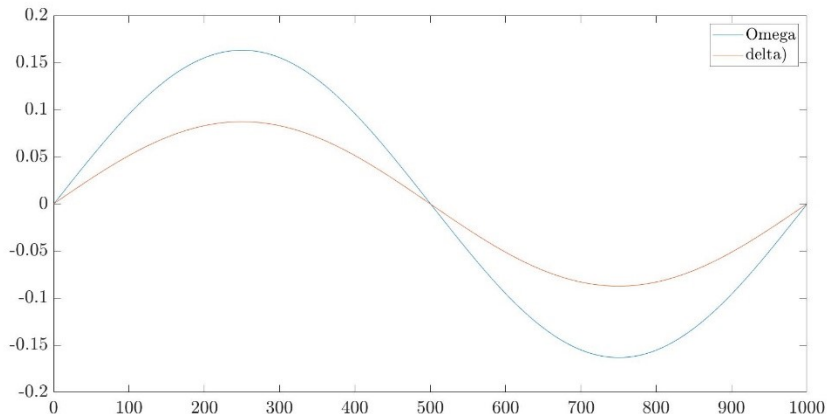


Fig. 27 Omega vs Delta for maneuver 2

- **Exercise 1.3: - Sine steer maneuver 3**

Conditions:  $u=100\text{Km/h}$  and  $\delta_{DO} = 5^\circ$

I used the simulation run time of 1000 and frequency of 0.001Hz for this exercise. The handling diagram at this condition is depicted in Fig. 28.

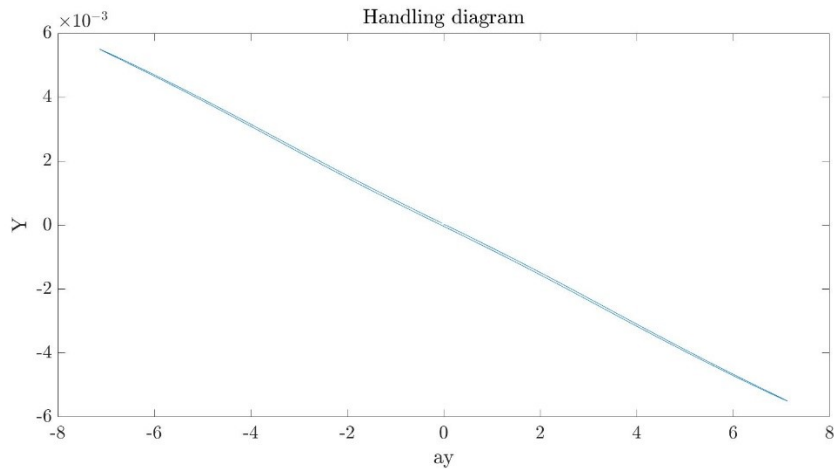


Fig. 28 Handling Diagram of maneuver 3

The curve is of the form of an ellipse going downwards, so the vehicle has oversteering behaviors as the previous case, but the value of handling behavior( $Y$ ) has increased from the previous case because speed and yaw rate are increased. It can also be observed from the coefficients value. Since  $a_y$  is small, the handling diagram can be approximated with a line.

$$Y = c_1 a_y + c_2$$

In this case,  $c_1 = -0.776546 \times 10^{-3}$  and  $c_2 = -0.0000245 \times 10^{-3}$

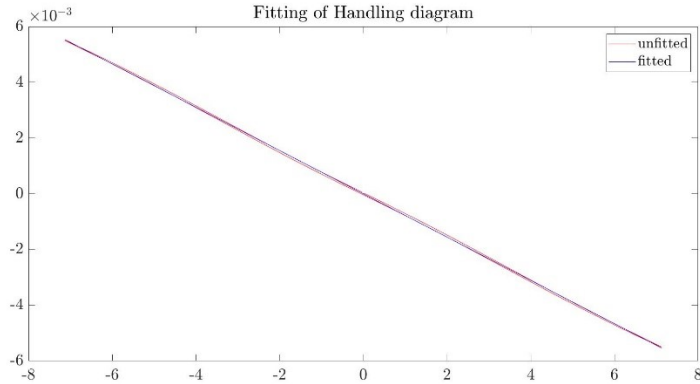


Fig. 26 Handling Diagram fitting of maneuver 3

The fitting curve is depicted in Fig. 26. From the fitted line we can depict that for left steer (positive  $a_y$ ), the vehicle is in oversteering condition. For right steer (negative  $a_y$ ), the vehicle is in understeering condition. The resulting curve of the handling diagram does not pass through the origin (when  $a_y = 0$  condition). The value of Y has increased furthermore than the previous case because  $a_y$  and the coefficients have increased. Hence, the effect can be observed in huge tracking error now and the vehicle never followed the desired maneuver. It can be seen in Fig. 27.

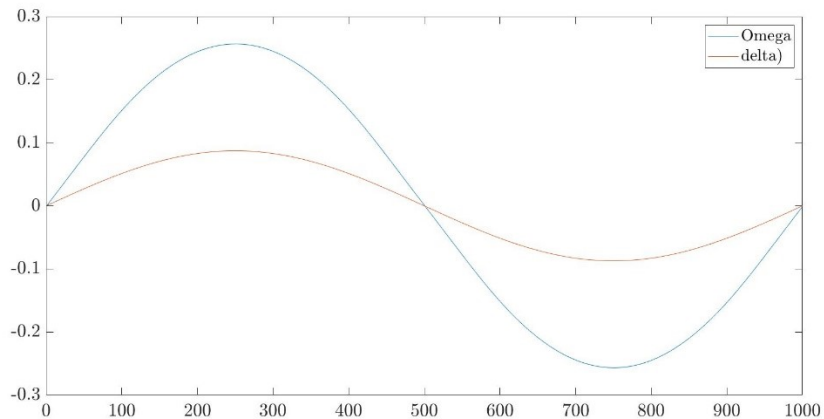


Fig. 27 Omega vs Delta for maneuver 3

## 4.2 Exercise 1.2: - Sine steer maneuvers

- **Exercise 1.1: - Sine steer maneuver 1**

Conditions:  $u=50\text{Km/h}$  and  $\delta_{D0} = 70^\circ$

I used the simulation run time of 1000 and frequency of 0.001Hz for this exercise. The handling diagram at this condition is depicted in Fig. 28. The graph is clearly nonlinear.

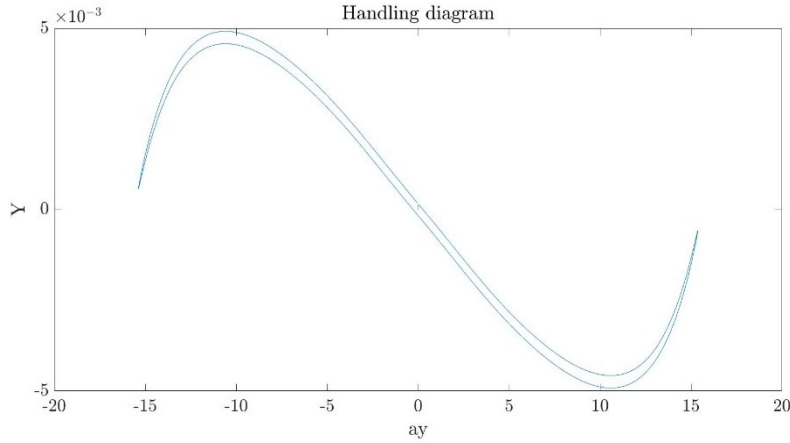


Fig. 28 Handling Diagram of maneuver 1

The steering behavior has changed from the previous case, it has both understeer as well as oversteer behavior. In this case high lateral accelerations are there, for high steering values. The oversteering behavior is reduced for higher lateral accelerations. The fitted curve is cubic for this case as shown in Fig.29.

$$Y = c_1 a_y + c_2 a_y^2 + c_3 a_y^3 + c_4$$

In this case,  $c_1 = -0.751865 X 10^{-3}$ ,  $c_2 = 0.000003 X 10^{-3}$ ,  $c_3 = 0.002863 X 10^{-3}$  and  $c_4 = -0.00000001 X 10^{-3}$

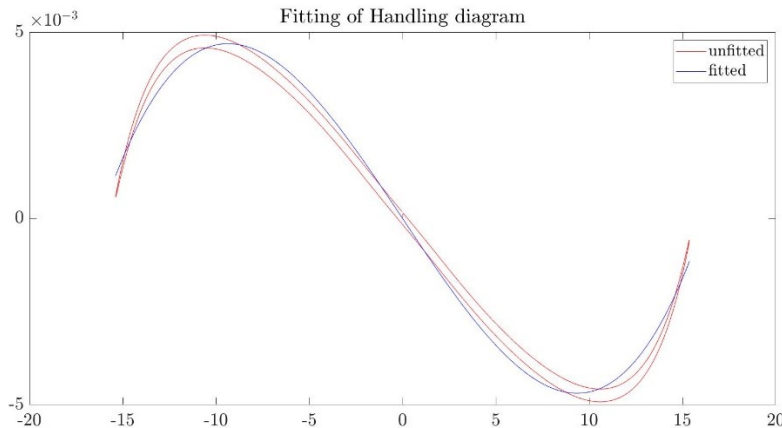


Fig. 29 Handling Diagram fitting of maneuver 1

The vehicle speed of the vehicle is less, so the yaw rate changes are also low, and the vehicle is almost able to follow the input steering. It can be seen in Fig. 30.

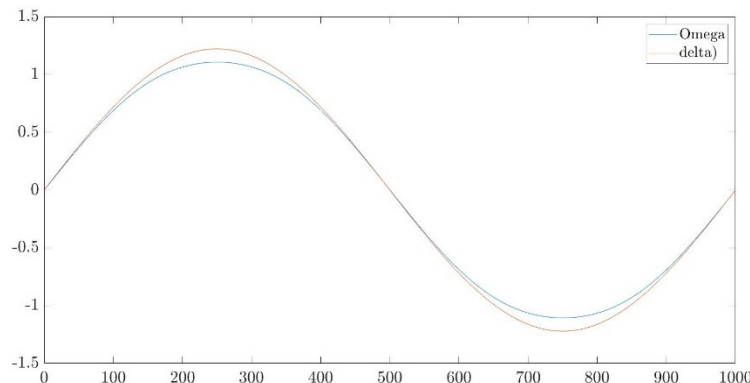


Fig. 30 Omega vs Delta for maneuver 1

- **Exercise 1.1: - Sine steer maneuver 2**

Conditions:  $u=80\text{Km/h}$  and  $\delta_{D0} = 24^\circ$

I used the simulation run time of 1000 and frequency of 0.001Hz for this exercise. The handling diagram at this condition is depicted in Fig. 28. The graph is clearly nonlinear.

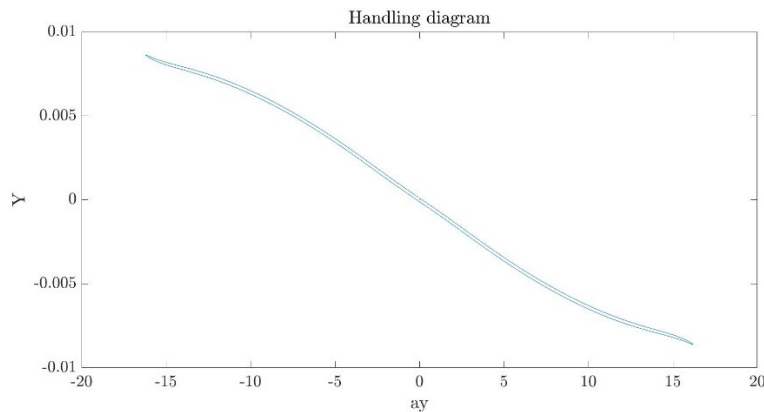


Fig. 28 Handling Diagram of maneuver 2

The steering behavior has changed from the previous case, it has both understeer as well as oversteer behavior. In this case high lateral accelerations are there, for medium steering values. The value of Y is also higher than that of the previous case. The fitted curve is cubic for this case as shown in Fig.29.

$$Y = c_1 a_y + c_2 a_y^2 + c_3 a_y^3 + c_4$$

In this case,  $c_1 = -0.7092813 \times 10^{-3}$ ,  $c_2 = 0.0000037 \times 10^{-3}$ ,  $c_3 = 0.0007186 \times 10^{-3}$  and  $c_4 = -0.00000001 \times 10^{-3}$

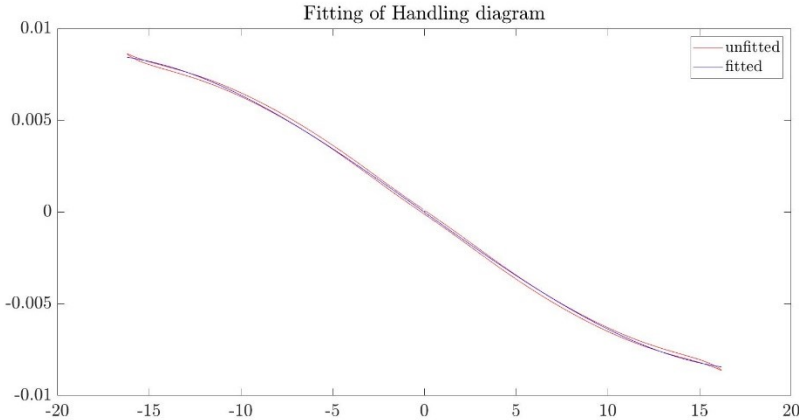


Fig. 29 Handling Diagram fitting of maneuver 2

The vehicle speed of the vehicle is higher, so the yaw rate changes are also higher than the previous case, and the vehicle is almost able to follow the input steering, oversteering in case of left turn and understeering in case of a right turn. It can be seen in Fig. 30.

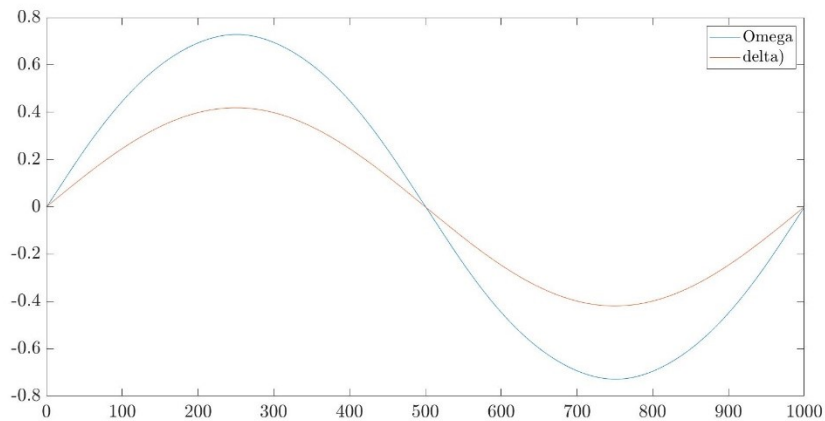


Fig. 30 Omega vs Delta for maneuver 2

- **Exercise 1.1: - Sine steer maneuver 3**

Conditions:  $u=100\text{Km/h}$  and  $\delta_{D0} = 12^\circ$

I used the simulation run time of 1000 and frequency of 0.001Hz for this exercise. The handling diagram at this condition is depicted in Fig. 30. The graph is clearly nonlinear.

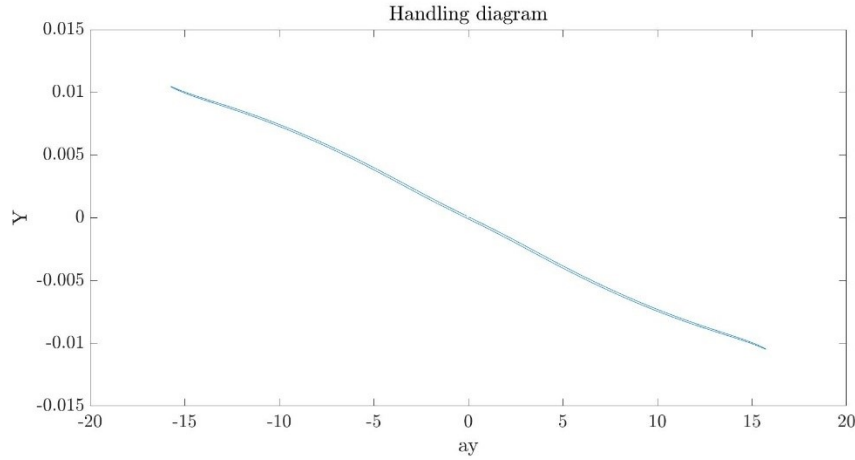


Fig. 31 Handling Diagram of maneuver 3

The value of  $Y$  is higher than that of the previous case. The fitted curve is cubic for this case as shown in Fig.32.

$$Y = c_1 a_y + c_2 a_y^2 + c_3 a_y^3 + c_4$$

In this case,  $c_1 = -0.787073 \times 10^{-3}$ ,  $c_2 = 0.0000049 \times 10^{-3}$ ,  $c_3 = 0.0005286 \times 10^{-3}$  and  $c_4 = -0.00000001 \times 10^{-3}$

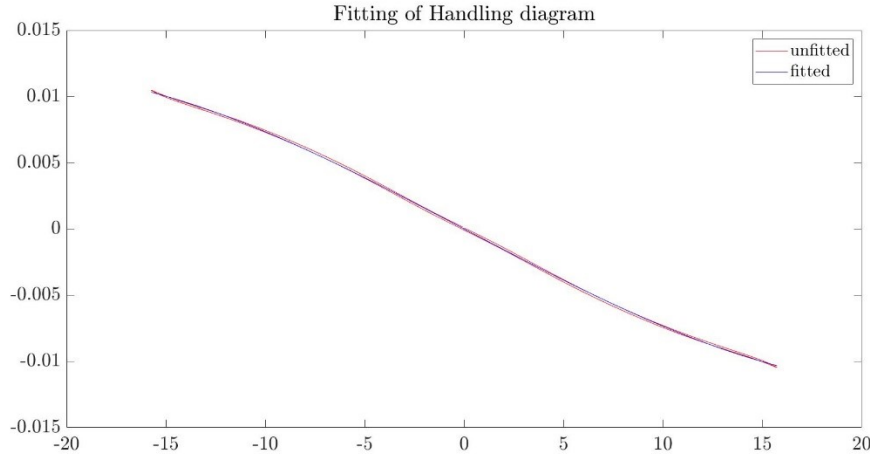


Fig. 32 Handling Diagram fitting of maneuver 3

The vehicle speed of the vehicle is higher, so the yaw rate changes are also higher than the previous case, and the vehicle is almost able to follow the input steering at all. It can be seen in Fig. 33.

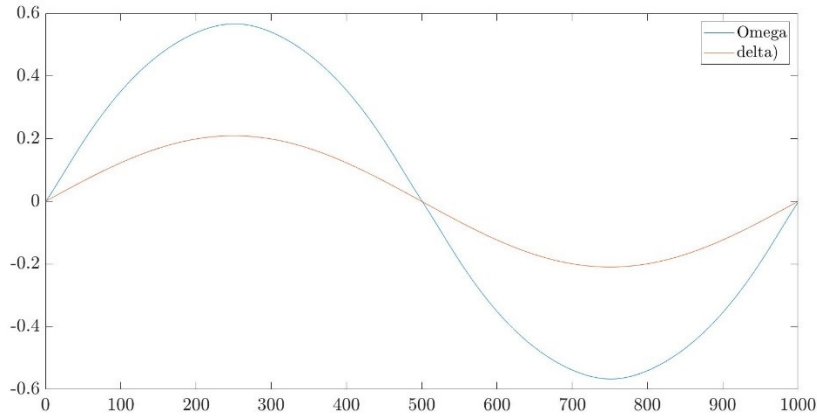


Fig. 33 Omega vs Delta for maneuver 3

### 4.3 Exercise 2: - Constant steer maneuvers

- **Exercise 2.1: - Constant steer maneuver 1**

Conditions:  $u_i = 20\text{Km/h}$ ,  $u_f = 40\text{Km/h}$  and  $\delta_{D0} = 10^\circ$

Observing the handling diagram in Fig. 34, for lateral accelerations greater than 0.4 the vehicle is in slight oversteering condition. The speed of the vehicle was made to increase gradually from 20 to 40 km/hr to maintain the steady state condition as seen in the velocity profile in Fig. 35. The vehicle is made to cover more than 1 round for the circular path so that we can observe the full real path of the vehicle.

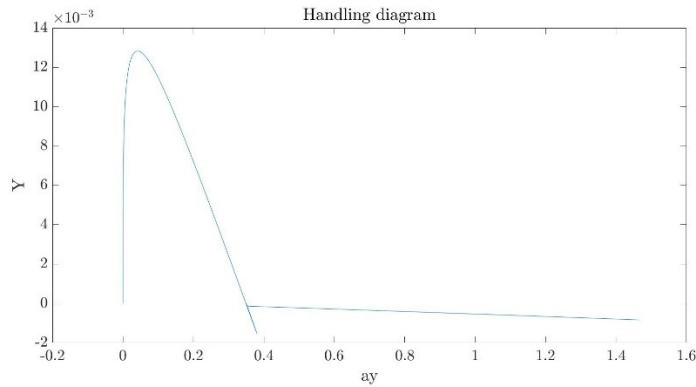


Fig. 34 Handling Diagram fitting of maneuver 1

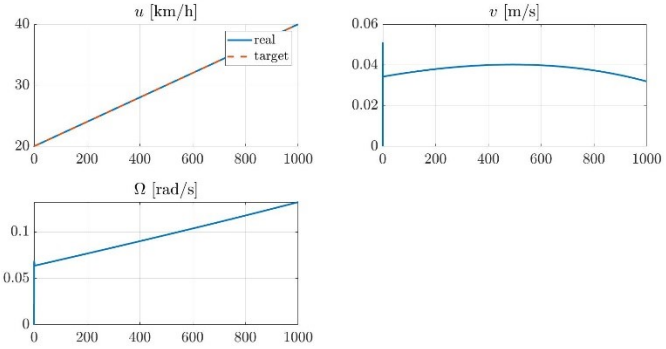


Fig. 35 Speed profile of maneuver 1

Observing the real path in Fig.36, if we observe the point (0,0), we clearly see that the vehicle is not able to reach the starting condition even after giving a constant steering. It reaches at a state with some positive value of  $y$ , which clearly means that the vehicle is oversteering in this maneuver.

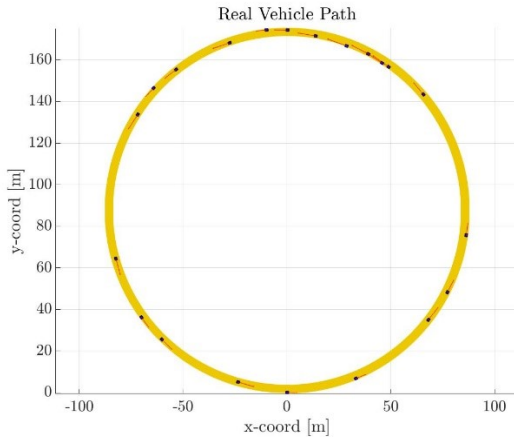


Fig. 36 Real vehicle path for maneuver 1

### ○ Exercise 2.2: - Constant steer maneuver 2

Conditions:  $u_i = 50\text{Km}/\text{h}$ ,  $u_f = 80\text{Km}/\text{h}$  and  $\delta_{D0} = 24^\circ$

Observing the handling diagram in Fig. 34, for lateral accelerations greater than 6 the vehicle is in slight oversteering condition. As the steering angle value is higher the lateral acceleration value is also higher in this case. The speed of the vehicle was made to increase gradually from 50 to 80 km/hr to maintain the steady state condition as seen in the velocity profile in Fig. 38. The vehicle is made to cover more than 1 round for the circular path so that we can observe the full real path of the vehicle.

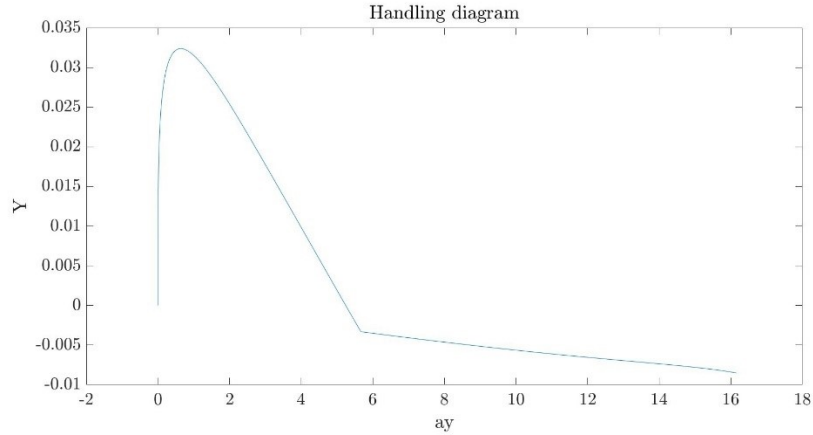


Fig. 37 Handling Diagram fitting of maneuver 2

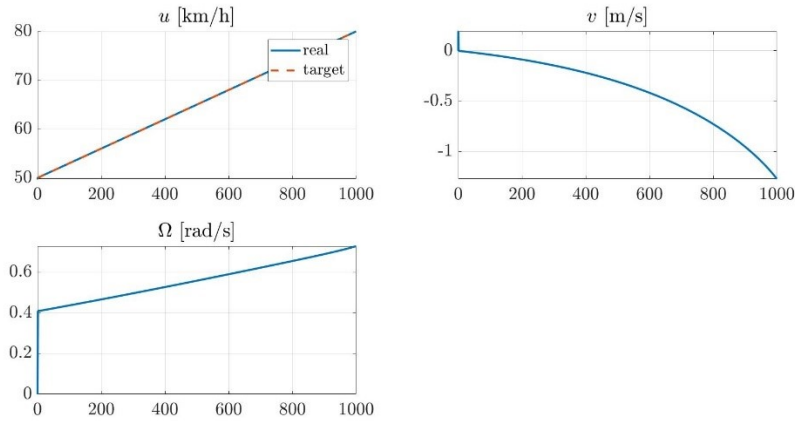


Fig. 38 Speed profile of maneuver 2

Observing the real path in Fig.36, if we observe the point (0,0), we clearly see that the vehicle is not able to reach the starting condition even after giving a constant steering. It reaches at a state with some positive value of  $y$ , which clearly means that the vehicle is oversteering in this maneuver. The value of  $y$  is higher than the previous case after completing the track due to higher speed and more steering angle value.

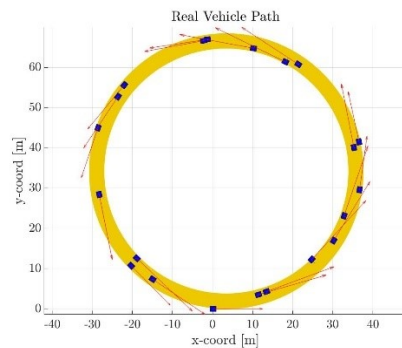


Fig. 39 Real vehicle path for maneuver 2

- **Exercise 2.3: - Pros and Cons**

Constant steer maneuvers	Sine steer maneuvers
Can be implemented by real drivers.	Very difficult to implement by real driver.
Robot not necessary for this test.	Need a robot to do this test
Can provide feedback only for either left or right turns	Can provide feedback for both left and right turns
Behavior can be analyzed either in positive or negative lateral accelerations	Behavior can be analyzed in positive and negative lateral accelerations
Can be tested at high steering angle values and steady state can be maintained	Difficult to maintain high angles and difficult to maintain steady state due to small frequency.

## 5. Assignment 5

### 5.1 Exercise 1: - Lateral Control

- **Exercise 1.1: - Clothoid-based lateral controller.**

In Clothoid-based lateral controller, the steering angle computation is given by the following equation.

$$\delta(s) = k(s) (L + K_{us}u^2)$$

It clearly depends upon the lookahead value  $L$ , lateral speed  $u$  and  $K_{us}$  the understeer gradient. These parameters play a crucial role in the performance of the controller. We already calculated  $K_{us}$  in the previous exercise. In this exercise, I tried different values of speed, the calculated  $K_{us}$  for that speed and the lookahead distance as seen in Table 1. We can clearly observe that the error is minimum at the lower speeds such as 30 Km/hr. Also, the value of error is lower with smaller lookahead value.

Speed (Km/hr)	$K_{us} \times 10^{-3}$	Lookahead	Max error(m)	Mean error(m)	Std. Deviation
30	-0.519059	10	0.4210	0.0805	0.104
30	-0.519059	5	0.1593	0.0395	0.0335
60	-0.639466	10	11.6229	4.1112	3.6427
60	-0.639466	5	4.6285	1.6100	1.6934
90	-0.744198	4	5.7237	0.7496	1.3449

Table 1. Comparison of Clothoid-based lateral controller in different conditions.

The tracking error and the real vehicle path is depicted in Fig. 41, 42, 43 and 45. It can be clearly observed that the vehicle can only take this steer maneuvers at low speed such as 30 Km/hr with low tracking errors. At higher speeds such as 90 km/hr, the tracking error and path tracking is very poor.

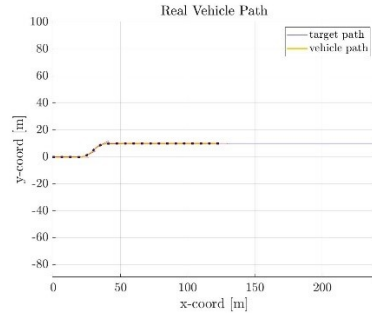


Fig. 40 Real vehicle path for  $u = 30\text{km/hr}$  and lookahead 5

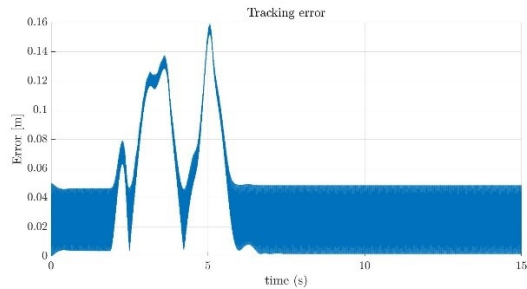


Fig. 41 Tracking error for  $u = 30\text{km/hr}$  and lookahead 5

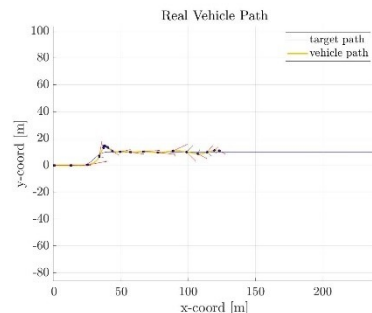


Fig. 42 Real vehicle path for  $u = 60\text{km/hr}$  and lookahead 5

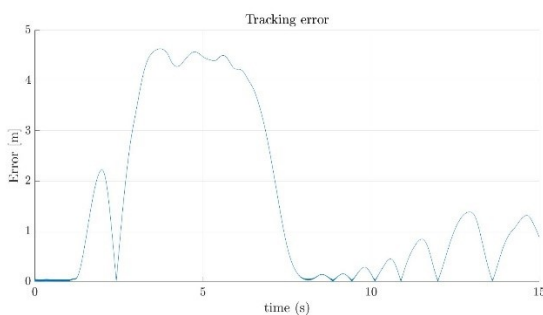


Fig. 43 Tracking error for  $u = 60\text{km/hr}$  and lookahead 5

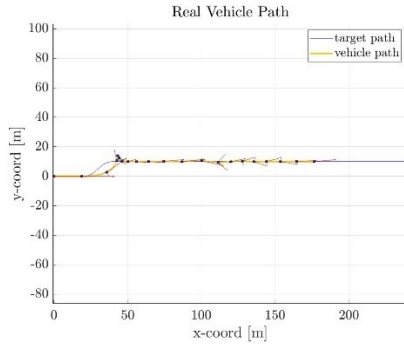


Fig. 44 Real vehicle path for  $u = 90\text{km/hr}$  and lookahead 5

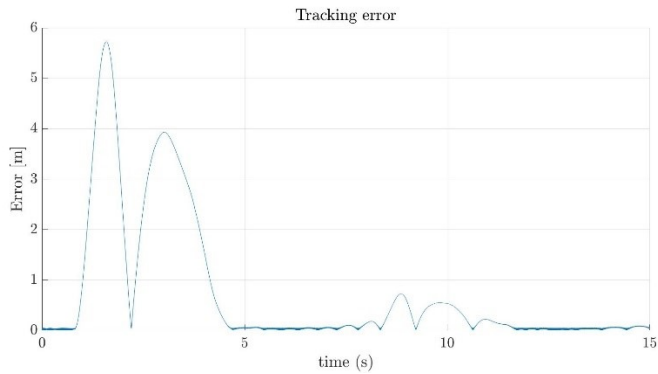


Fig. 45 Tracking error for  $u = 90\text{km/hr}$  and lookahead 4

- **Exercise 1.2: - Pure pursuit controller**

In Pure pursuit controllers, the steering angle computation is given by the following equation.

$$\delta = \arctan(L/R)$$

here R is arc radius and is given by:

$$R = (x^2 + y^2)^{1/2} / 2 \sin(\lambda)$$

In this controller lookahead distance is the tunable coefficient depending on the vehicle velocity. The performance at low speeds is good with lower lookahead distance and at higher speed the value of the lookahead distance should be increased above a certain threshold to achieve satisfactory results. This is depicted in Table 2. The real vehicle path for the best lookahead distance in Table 2 with speeds 30km/hr and 60km/hr is shown in Fig 46, 47, 48 and 49. The performance of the controller is better at lower speed is better than at higher speeds. But Clothoid-based controller performance is better for all the cases if it is tuned properly.

Speed (Km/hr)	Lookahead	Max error(m)	Mean error(m)	Std. Deviation
30	10	1.0151	0.1767	0.2550
30	5	0.1832	0.0450	0.04298
60	15	7.7270	0.3197	0.8194
60	5	16.0253	6.6502	5.1990

Table 2. Comparison of Pure pursuit controllers in different conditions

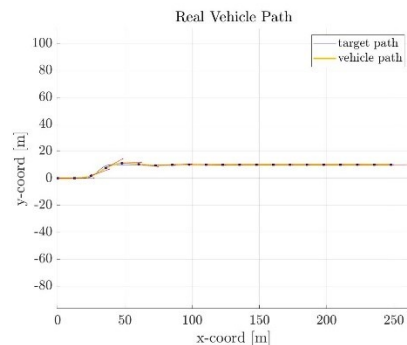


Fig. 46 Real vehicle path for  $u = 30\text{km/hr}$  and lookahead 5

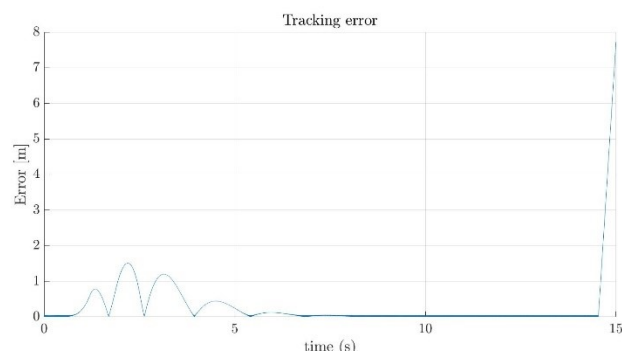


Fig. 47 Tracking error for  $u = 30\text{km/hr}$  and lookahead 5

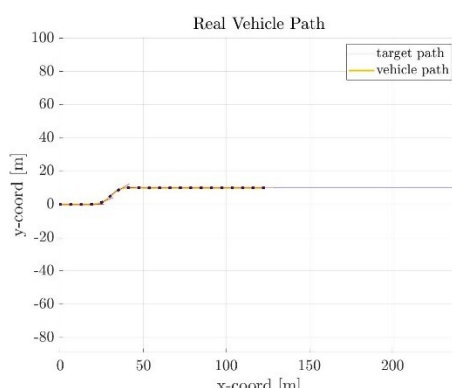


Fig. 48 Real vehicle path for  $u = 60\text{km/hr}$  and lookahead 15

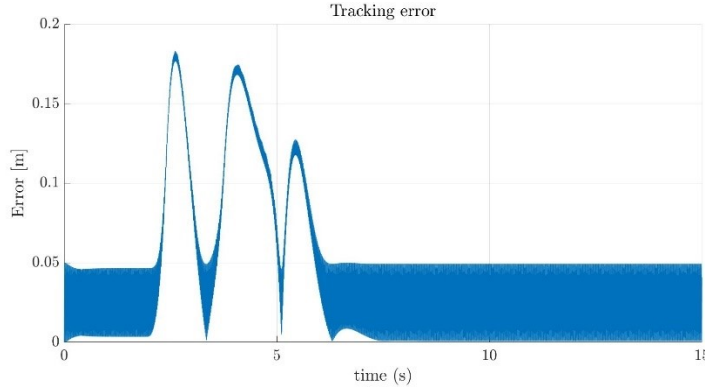


Fig. 49 Tracking error for  $u = 60\text{km/hr}$  and lookahead 15

- **Exercise 1.3: - Stanley kinematic controllers**

In Stanley kinematic controllers, the steering angle computation is given by the following equation.

$$\delta = \Delta\theta + \arctan(k_e e/v_f)$$

In this controller  $k_e$  is the tunable coefficient. The values of the  $\delta$  are saturated at  $\delta_{\min}$  for negative values and  $\delta_{\max}$  for positive values. The controller gains need to be tuned properly for each speed. This can be seen in the Table 3. At low speed, the gain should be set higher and at higher speeds lower gains give better performance. The performance of this controller is comparable Clothoid-based controllers for medium speed of 60 km/hr. The real vehicle path for the best gains in Table. 3 with speeds 30km/hr and 60km/hr is shown in Fig 50, 51, 52 and 53.

Speed (Km/hr)	$K_e$	Max error(m)	Mean error(m)	Std. Deviation
30	0.5	0.9873	0.1847	0.2387
30	0.1	1.0088	0.1516	0.2593
60	0.5	5.8930	1.1919	1.5298
60	0.1	5.8371	2.3353	1.1428

Table 3. Comparison of Stanley kinematic controllers in different conditions

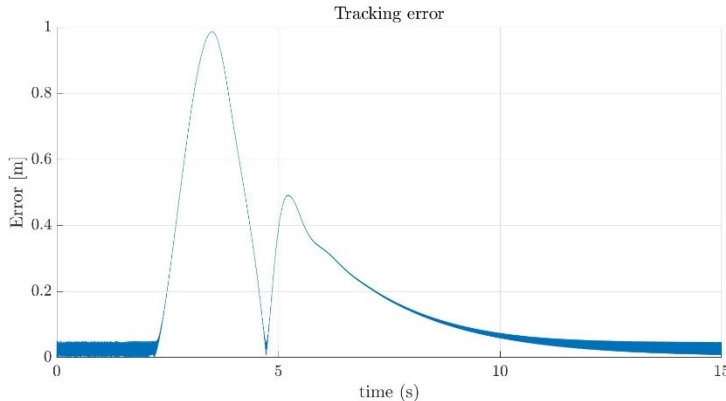


Fig. 50 Tracking error for  $u = 30\text{km/hr}$  and  $k_e = 0.5$

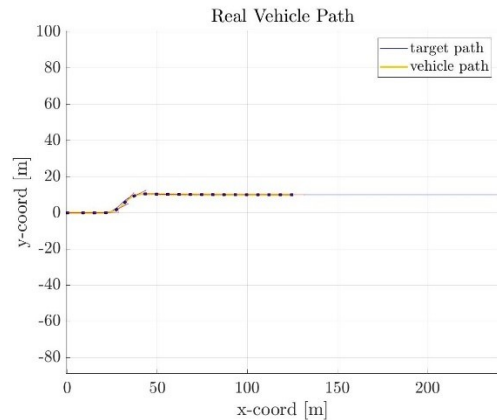


Fig. 51 Real vehicle path for  $u = 30\text{km/hr}$  and  $k_e = 0.5$

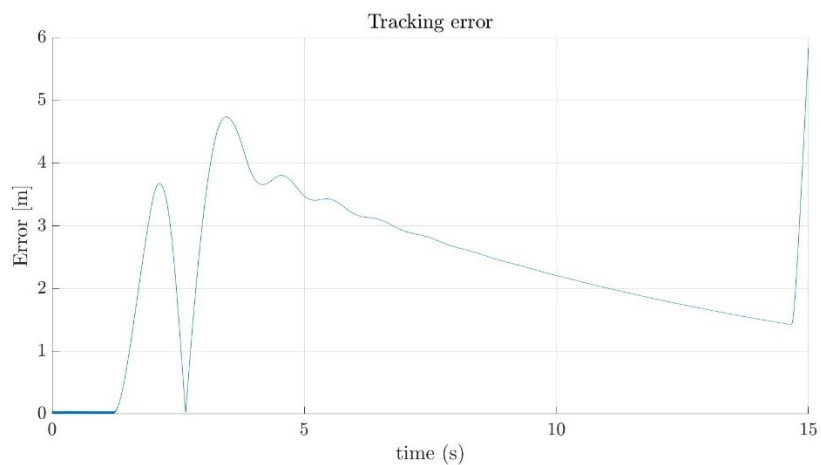


Fig. 52 Tracking error for  $u = 60\text{km/hr}$  and  $k_e = 0.1$

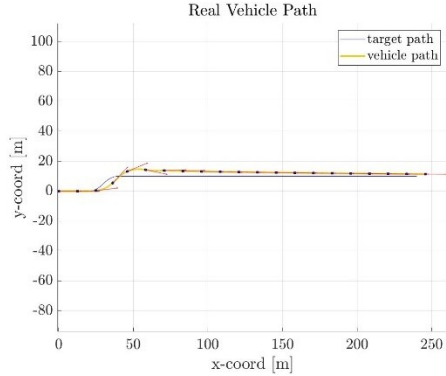


Fig. 53 Real vehicle path for  $u = 60\text{km/hr}$  and  $k_e = 0.1$

- **Exercise 1.4: - Stanley dynamic controllers**

In Stanley kinematic controllers, the steering angle computation is given by the following equation.

$$\delta = \Delta\theta + \arctan(k_e \cdot e/v_f) + k_y(\Omega_t - \Omega)$$

In this controller  $k_y$  and  $k_e$  are the tunable coefficient. The values of the  $\delta$  are saturated at  $\delta_{\min}$  for negative values and  $\delta_{\max}$  for positive values. In the equation,  $\Omega_t = v_f k$  being the trajectory yaw rate and  $k$  being the local path curvature. The controller gains can be kept similar compared to the Stanley kinematic controller. This can be seen in the Table 4. The performance of this controller is better than the Stanley kinematic controller for low speed of 30 km/hr. The real vehicle path for the best gains in Table. 3 with speeds 30km/hr and 60km/hr is shown in Fig 54, 55, 56 and 57.

Speed (Km/hr)	$K_e$	$K_y$	Max error(m)	Mean error(m)	Std. Deviation
30	0.2	0.2	0.6743	0.1502	0.1906
30	0.1	0.1	0.6619	0.0974	0.1720
60	0.2	0.2	7.2593	0.4327	0.9525
60	0.1	0.1	6.4432	0.6919	0.9947

Table 4. Comparison of Stanley dynamic controllers in different conditions

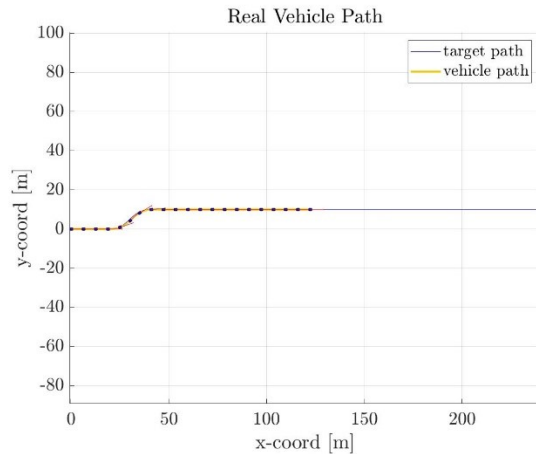


Fig. 54 Real vehicle path for  $u = 30\text{km/hr}$  and  $k_e, k_y = 0.1$

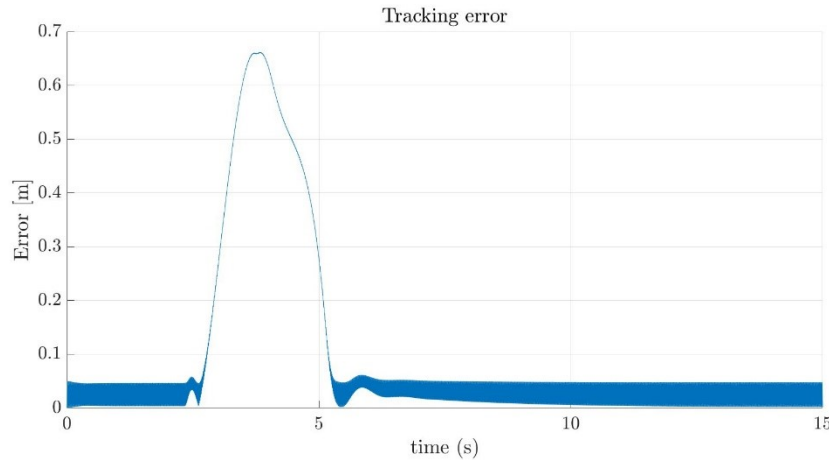


Fig. 55 Tracking error for  $u = 30\text{km/hr}$  and  $k_e, k_y = 0.1$

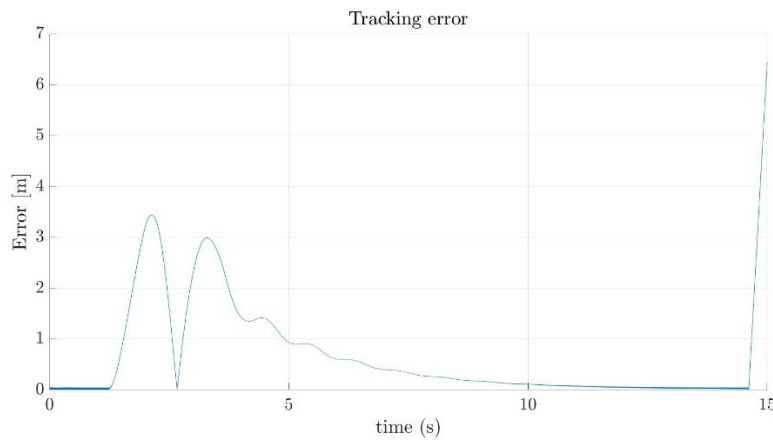


Fig. 56 Tracking error for  $u = 60\text{km/hr}$  and  $k_e, k_y = 0.1$

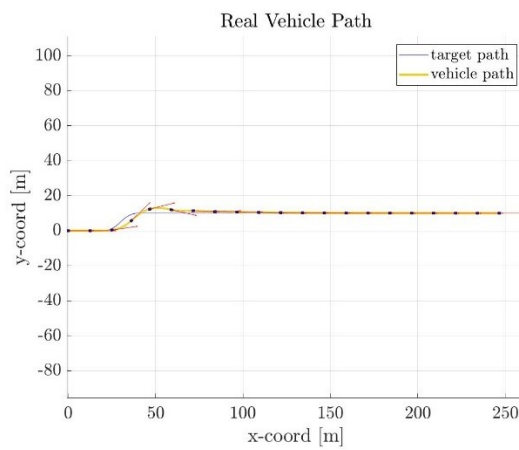


Fig. 57 Real vehicle path for  $u = 60\text{km/hr}$  and  $k_e, k_y = 0.1$

- **Exercise 1.5: - Pros and cons**

**Clothoid controller:**

**PROS**

- More accurate than other controllers.
- Can compute the curve at high speeds.
- Smooth and precise curvature.
- More realistic as the steering behavior is considered.

**CONS**

- Computationally expensive
- Need different lookahead at different speeds.
- Performance is poor for high speeds.

**Pure Pursuit controller:**

**PROS**

- Easy to implement and easy to compute the steering angle.
- Path smoothness is high.
- Partially works well for high speeds.

**CONS**

- Different Look ahead setting required for different speeds.
- Acceptable results only for low speeds.

**Stanley Kinematic controller**

**PROS**

- Very low computation cost with medium range performance
- Easy to implement.

**CONS**

- Cannot be used for high speeds.
- Gains need to be tuned.

**Stanley Dynamic controller**

**PROS**

- Works good with low-speed performance.
- Easy to implement.

**CONS**

- Higher number of parameters
- More computation than Stanley kinematic controllers.
- Cannot be used for high speeds.

# 6. Assignment 6

## 6.1 Exercise 1: - Route planning

- **Exercise 1.1: - Optimizing RRT\***

**Parameters:**

**Connection distance**- distance between two nodes

**Min Iterations** - Minimum number of iterations for RRT\* loop

**Max Iterations** - Maximum number of loops for RRT\*

**Interpolation distance** - Resampling the RRT\* points for path smoothness.

**Min Turn Radius** – Depends upon max steer angle.

Connection distance	Min Iterations	Max Iterations	Interpolation distance	Steering	Computation Time	Reachability
35	1e5	1e6	30	4	34.2	Yes
40	1e5	1e6	20	4	34.1	Yes
40	1e4	1e5	30	4	33.1	Yes
45	1e4	1e5	30	5	33.1	Yes
40	1e4	1e5	20	4	33.1	Yes

Table 5 RRT\* parameter optimization

I tried to change the parameters for RRT\*. If the interpolation distance is high, then the time to compute the path is also more. If the number of iterations is less then, the path generated is not as smooth as with a greater number of iterations. I also tried to change the steering angle, but the results were not good. So finally, I tuned the connection distance and the interpolation distance to get a smooth trajectory that the vehicle can follow. The best results were obtained for connection distance =40 and interpolation distance =20 with min iterations 1e4 and max iterations as 1e5 as shown in Fig. 58. Some of the other results are shown in Fig. 59, 60 and 61. Then I also saved the path for computation time saving.

## Path RRT\*

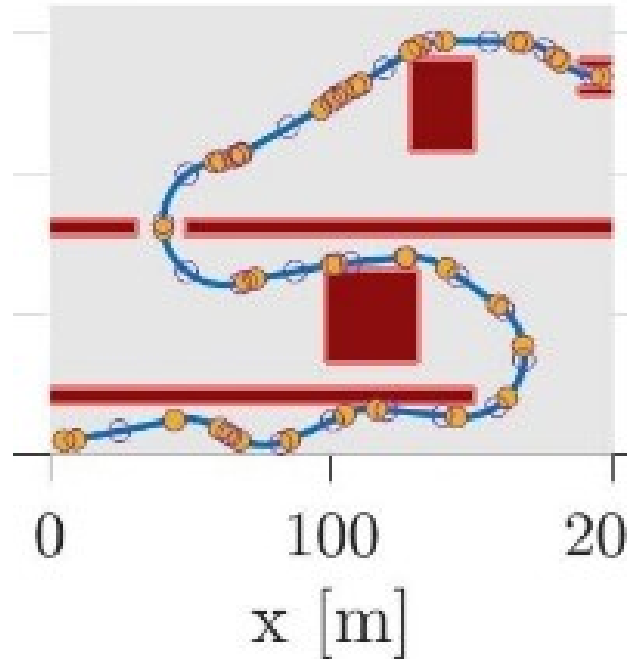


Fig. 58 RRT\* path with connection distance = 40 and interpolation distance =20

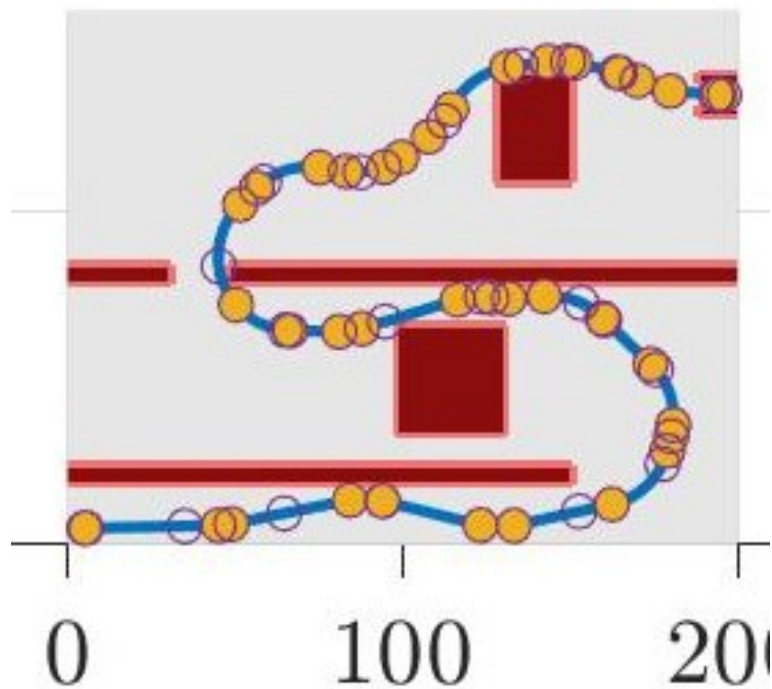


Fig. 59 RRT\* path with connection distance = 40 and interpolation distance =30

## Path RRT\*

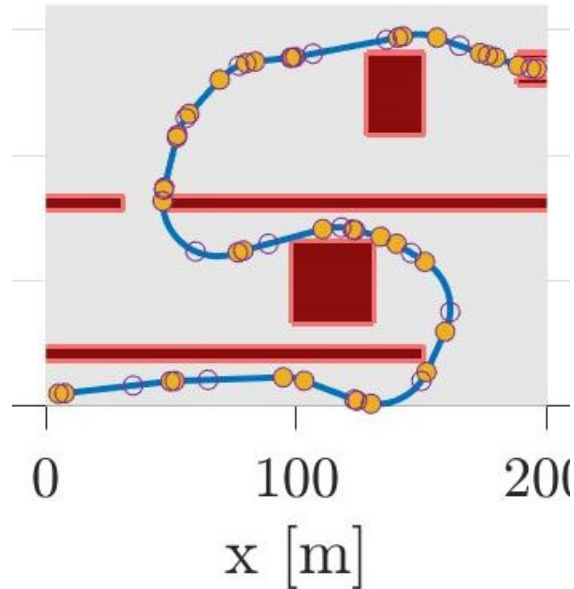


Fig. 59 RRT\* path with connection distance = 45, max steer angle =5 and interpolation distance = 30

## Path RRT\*

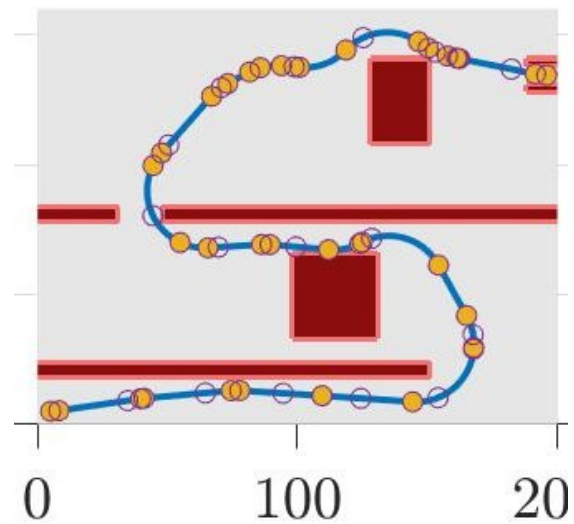


Fig. 59 RRT\* path with connection distance = 35 and interpolation distance = 30

- **Exercise 1.2: - Clothoid fitting vs dubins paths**

Then path generated by the global planner has less points and the local planner need to generate more points that can follow the vehicle kinematic and dynamic constraints. The path generated by clothoids is better than dubins. The major differences are mentioned in Table 6.

Clothoids	Dubins
Solves the problem considering curvature as a linear function of arclengths	Solves only for six configurations considering max turning radius.
The curvature generated is smooth	The curvature generated is not as smooth as clothoids
Less lateral jerks	More lateral jerks
Curvature $k(s) = k_1 + k_2 s$ $k_1$ = curvature at base point $k_2$ = sharpness	Curvature is only either of the three values [MAX, 0, +MAX]
Solved using both G1(1 arc) and G2(3 arcs) Hermite solvers	6 configurations are calculated, and the best id selected

Table 6. Clothoids vs Dubins

- **Exercise 1.2: - Efficiency of RRT\* for route planning and the limitations**

The plan generated by the RRT\* is not smooth but it is computationally very fast as seen in the previous section. This path can be easily chosen for global plan and RRT\* is usually chosen as the global planning algorithm. Clothoids can be used to smooth the path with the help of splines so that the continuity of the curves is maintained. This is shown in Fig. 62.

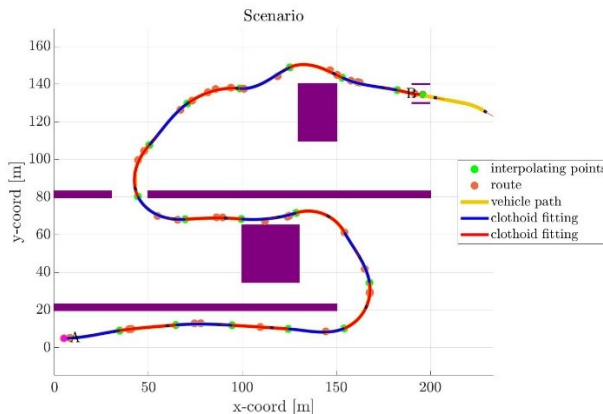


Fig. 62 RRT path in combination with clothoids at 20km/hr speed

As the speed is increased, the path required is smoother curves for the local planner to follow. This is depicted in Fig 63. This is one of the bottlenecks since the curvatures generated by RRT\* are not so smooth MPC is one of a good option which tries to reduce the speed when the curvature is very high. The path generated by MPC also provides smooth trajectory that the vehicle can follow. The comparison at various speed of different controllers with RRT\* planned path is done in the next section.

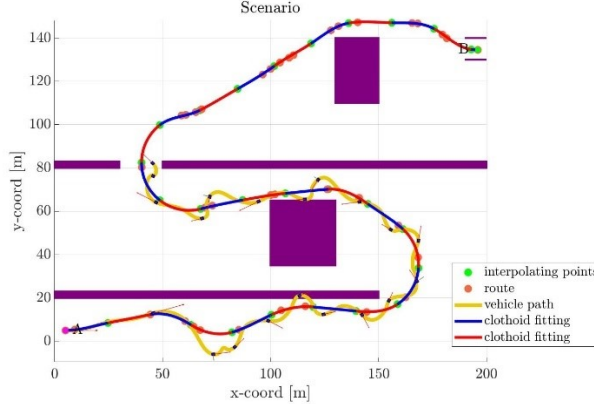


Fig. 63 RRT path in combination with clothoids at 60km/hr speed

## 6.2 Exercise 2: - Lateral Control

- **Exercise 2.1: - Clothoids Controller**

The path tracking of the Clothoids Controller is depicted in Table 7. The tracking errors, trajectory tracking, and the steering variations are depicted in Fig. 64, 65, 66, 67, 68, and 69. From the graphs we can clearly observe that the vehicle is very unstable at high speeds and the tracking error is also very high at higher speed levels. The error reduces with smaller lookahead values. The steering fluctuations are low at low speeds. The steering angle values are very high and the steering fluctuations are high as well at the high speeds to track the path.

Speed (Km/hr)	$K_{us} \times 10^{-3}$	Lookahead	Max error(m)	Mean error(m)	Std. Deviation
30	-0.519059	10	6.4146	1.9618	1.6228
30	-0.519059	5	6.3880	1.9673	1.6211
60	-0.639466	10	12.9373	2.9516	2.4093
60	--0.639466	5	10.5457	2.3788	1.8887

Table 7. Comparison of Clothoid-based lateral controller in different conditions.

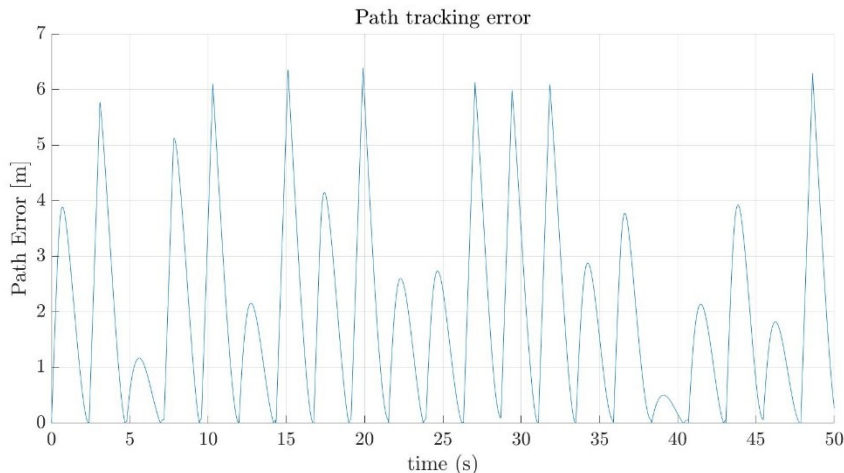


Fig. 64 Path tracking error with clothoids at 30km/hr speed and lookahead =5

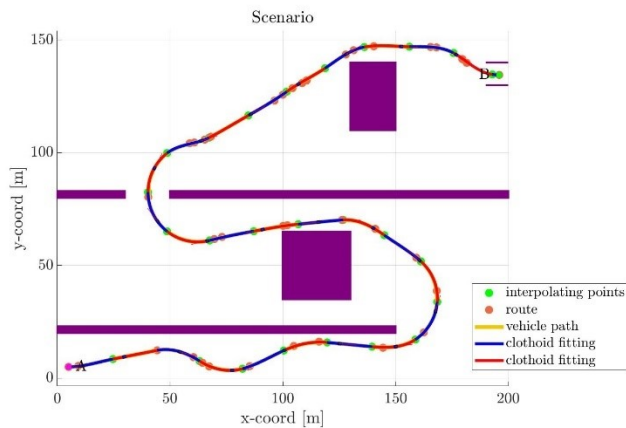


Fig. 65 Path tracking with clothoids at 30km/hr speed and lookahead =5

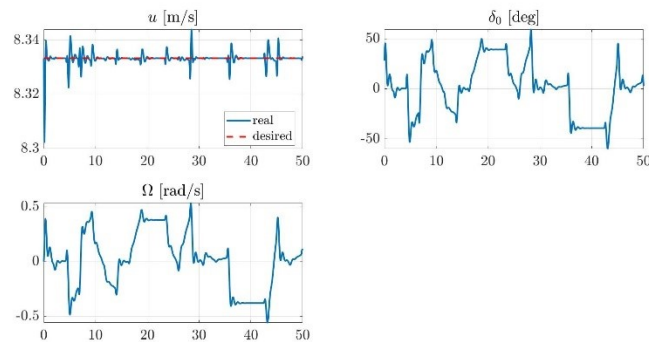


Fig. 66 Steering variation with clothoids at 30km/hr speed and lookahead =5

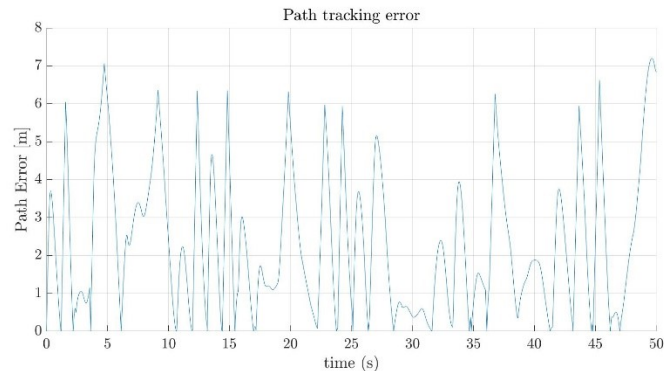


Fig. 67 Path tracking error with clothoids at 60km/hr speed and lookahead =5

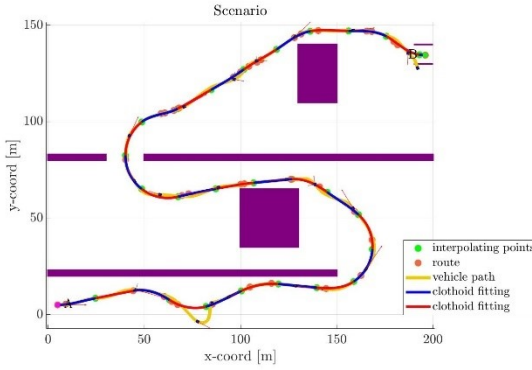


Fig. 68 Path tracking with clothoids at 60km/hr speed and lookahead =5

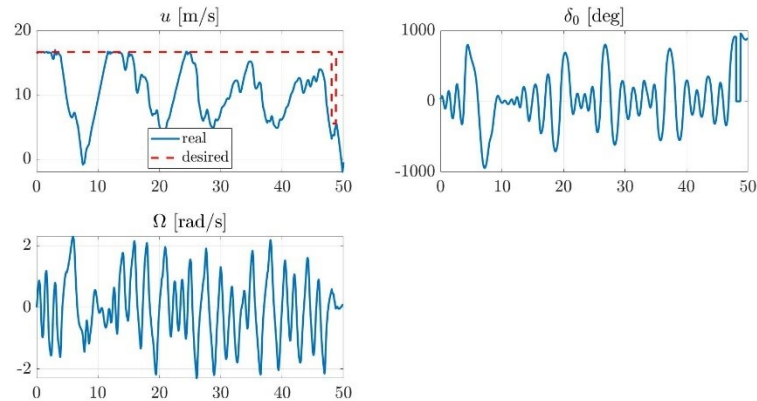


Fig. 69 Steering variation with clothoids at 60km/ hr speed and lookahead =5

- **Exercise 2.2: - Pure pursuit controller**

The path tracking of the Pure pursuit controller is depicted in Table 8. The tracking errors, trajectory tracking, and the steering variations are depicted in Fig. 70, 71, 72, 73, 74 and 75. From the graphs, we can clearly observe that the vehicle is very unstable at high speeds and rolls out in the track. The controller is not able to track the path at high speeds. For low speed, the performance is comparable to clothoids controller. The tracking error is also very high at higher speed levels due to the roll out. The error reduces slightly with smaller lookahead values at low speeds and changes drastically at high speeds. The steering fluctuations are low at low speeds. The steering angle values are high at high speeds.

Speed (Km/hr)	Lookahead	Max error(m)	Mean error(m)	Std. Deviation
30	10	6.4509	1.9347	1.6193
30	5	6.3772	1.9678	1.6193
60	15	23.1521	3.4866	4.4347
60	5	17.6475	4.8345	3.8004

Table 8 Comparison of Pure Pursuit lateral controller in different conditions

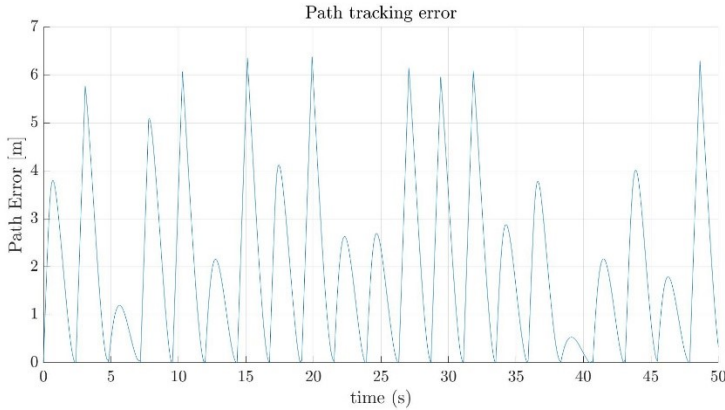


Fig. 70 Trajectory tracking error with pure pursuit controller at 30km/hr speed and lookahead =5

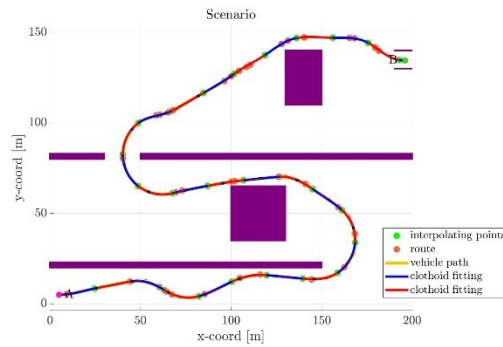


Fig. 71 Trajectory tracking with pure pursuit controller at 30km/hr speed and lookahead =5

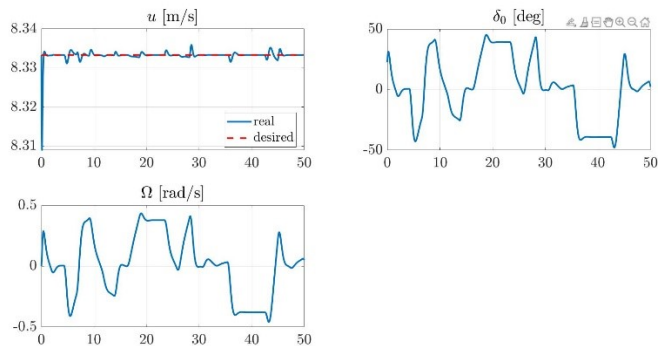


Fig. 72 Steering variation with pure pursuit controller at 30km/hr speed and lookahead =5

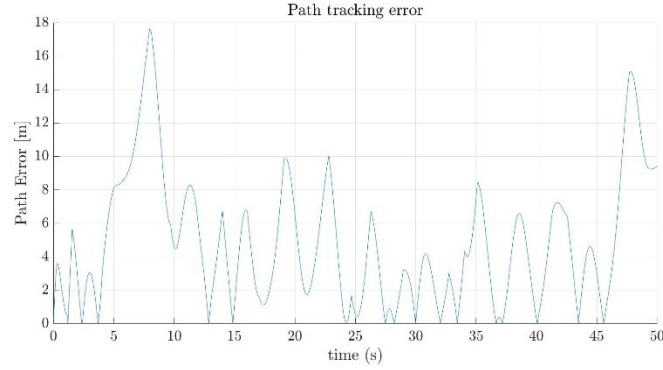


Fig. 73 Trajectory tracking error with pure pursuit controller at 60km/hr speed and lookahead =5

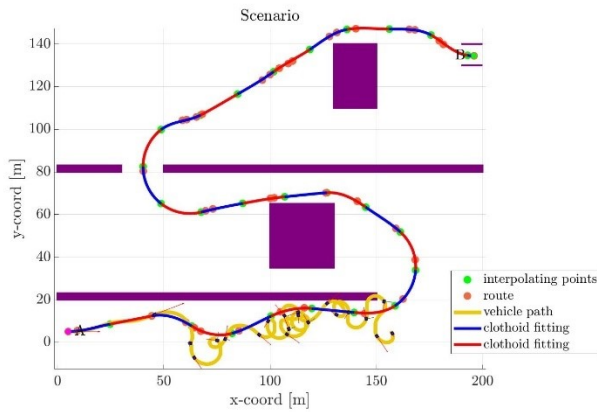


Fig. 74 Trajectory tracking with pure pursuit controller at 60km/hr speed and lookahead =5

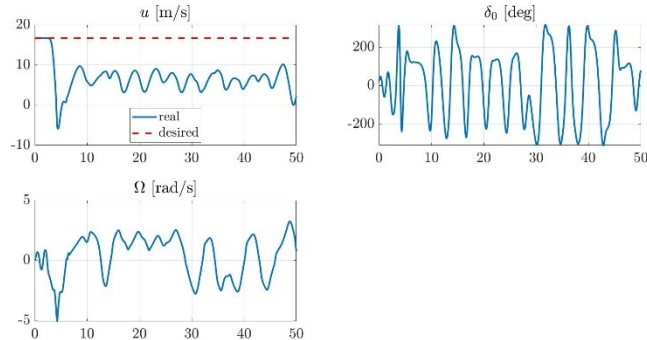


Fig. 75 Steering variation with pure pursuit controller at 60km/hr speed and lookahead =5

### ○ Exercise 2.3: - Stanley kinematic controllers

The path tracking of the Stanley kinematic controllers is depicted in Table 9. The tracking errors, trajectory tracking, and the steering variations are depicted in Fig. 76, 77, 78, 79, 80 and 81. From the graphs we can clearly observe that the vehicle is very unstable at high speeds and rolls out in the track. The controller is not able to track the path at high speeds. For low speed, the

performance is comparable to clothoids controller. The tracking error is also very high compared to Stanley dynamic controller. The error reduces slightly or remains same with smaller gain values at low speeds and at high speeds. The steering fluctuations are low at low speeds but very high at high speeds. The steering angle values are not very high at the high speeds compared to clothoids.

Speed (Km/hr)	$K_e$	Max error(m)	Mean error(m)	Std. Deviation
30	0.5	6.3591	1.9873	1.6081
30	0.1	6.3624	1.9987	1.5949
60	0.5	7.6871	2.3859	2.0692
60	0.1	7.6181	2.4981	2.0639

Table 9 Comparison of Stanley kinematic controllers in different conditions

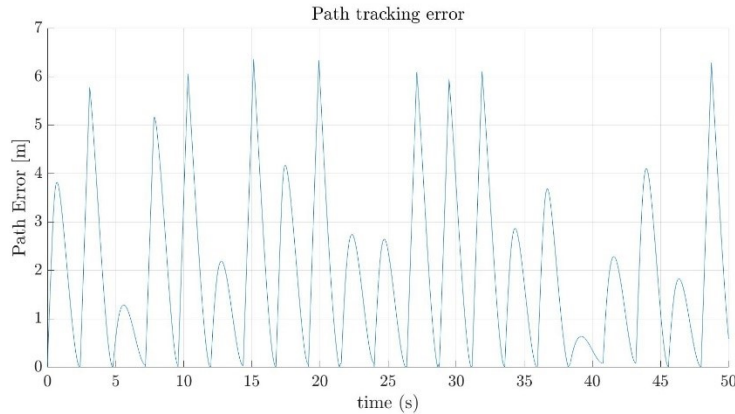


Fig. 76 Trajectory tracking error with Stanley kinematic controllers at 30km/hr speed and  $K_e = 0.5$

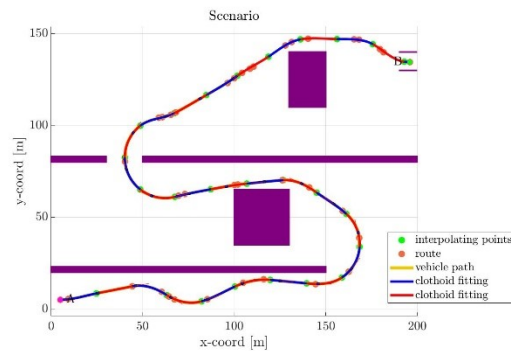


Fig. 77 Trajectory tracking with Stanley kinematic controllers at 30km/hr speed and  $K_e = 0.5$

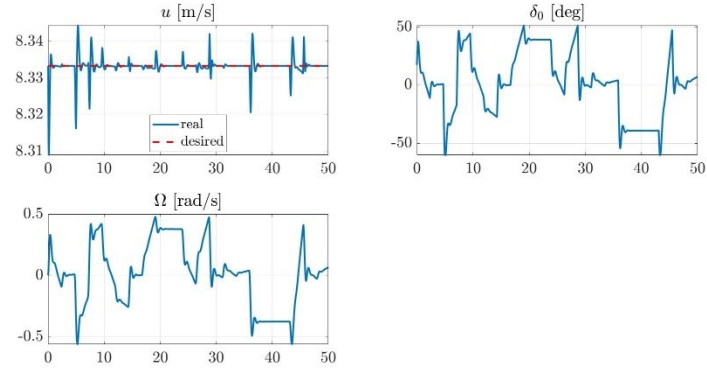


Fig. 78 Steering variation with Stanley kinematic controllers at 30km/hr speed and  $K_e = 0.5$

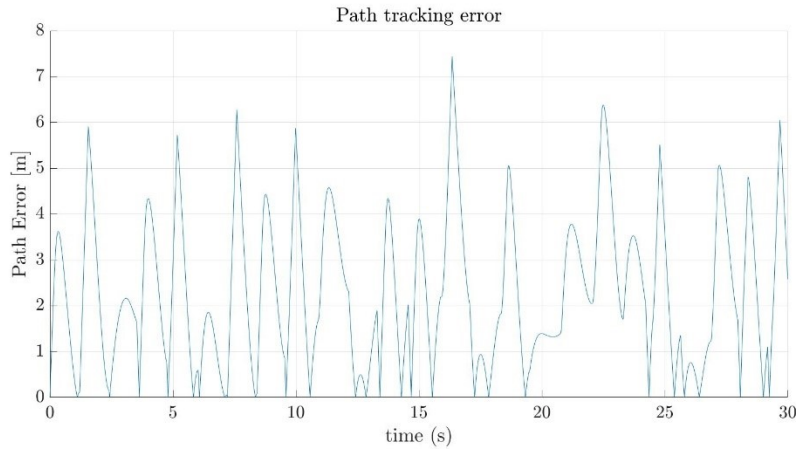


Fig. 79 Trajectory tracking error with Stanley kinematic controllers at 60km/hr speed and  $K_e = 0.1$

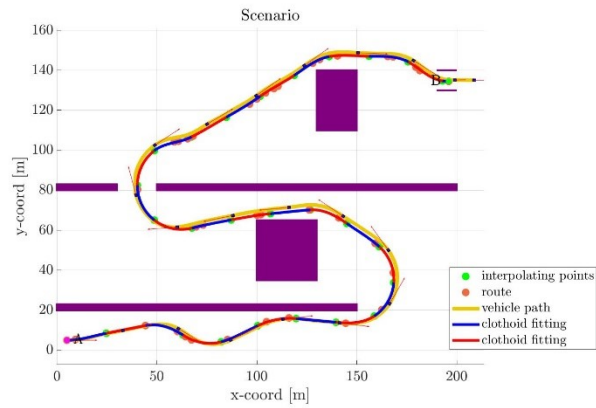


Fig. 80 Trajectory tracking error with Stanley kinematic controllers at 60km/hr speed and  $K_e = 0.1$

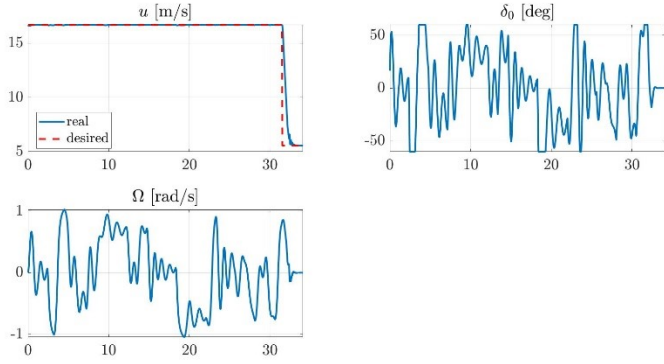


Fig. 81 Steering variation with Stanley kinematic controllers at 60km/hr speed and  $K_e = 0.1$

#### ○ Exercise 2.4: - Stanley dynamic controllers

The path tracking of the Stanley dynamic controllers is depicted in Table 10. The tracking errors, trajectory tracking, and the steering variations are depicted in Fig. 82, 83, 84, 85, 86 and 87. From the graphs we can clearly observe that the vehicle is unstable as some of the previous controllers. The error is high at high speeds. The controller can track the path to a certain extent at high speeds. For low speed, the performance of Stanley kinematic controller is slightly better. The error reduces slightly with smaller gains at low speeds and changes drastically at high speeds. The steering fluctuations are low at low speeds. The steering angle fluctuations are very high at high speeds. The controller performed the best for high speeds in comparison to others.

Speed (Km/hr)	$K_e$	$K_y$	Max error(m)	Mean error(m)	Std. Deviation
30	0.2	0.2	7.7159	2.6778	1.8683
30	0.1	0.1	6.9679	2.4208	1.7398
60	0.2	0.2	13.9746	5.7379	3.7081
60	0.1	0.1	7.3754	2.3670	1.6164

Table 10. Comparison of Stanley dynamic controllers in different conditions

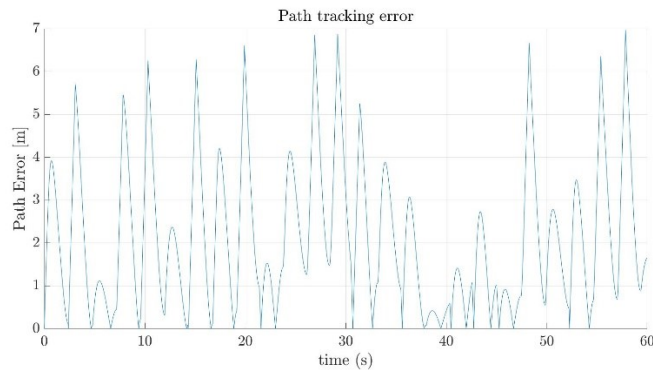


Fig. 82 Trajectory tracking error with Stanley dynamic controllers at 30km/hr speed and  $K_e, K_y = 0.1$

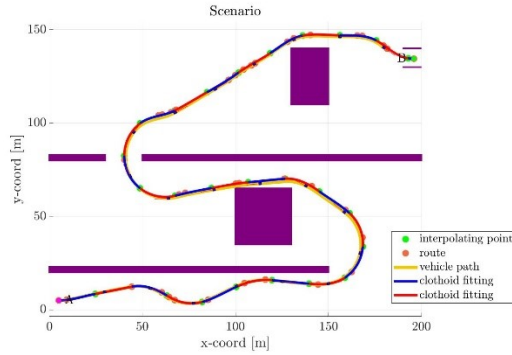


Fig. 83 Trajectory tracking with Stanley dynamic controllers at 30km/hr speed and

$$K_e, K_y = 0.1$$

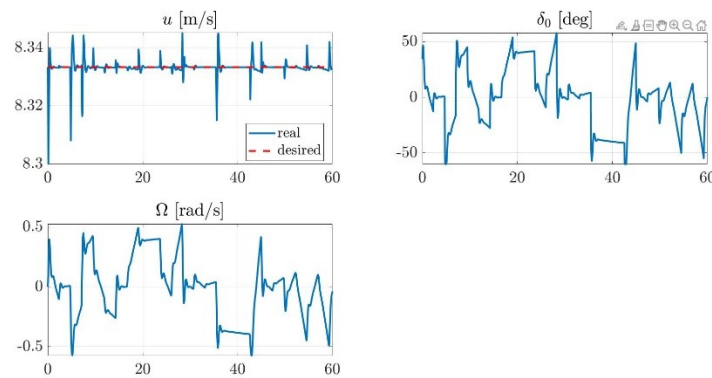


Fig. 84 Steering variation with Stanley dynamic controllers at 30km/hr speed and

$$K_e, K_y = 0.1$$

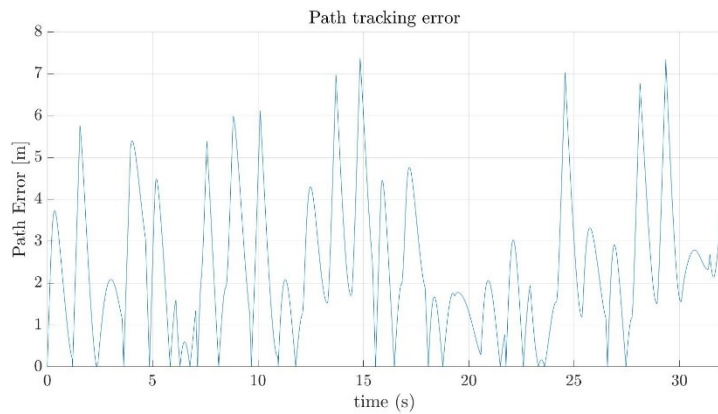


Fig. 85 Trajectory tracking with Stanley dynamic controllers at 60km/hr speed and

$$K_e, K_y = 0.1$$

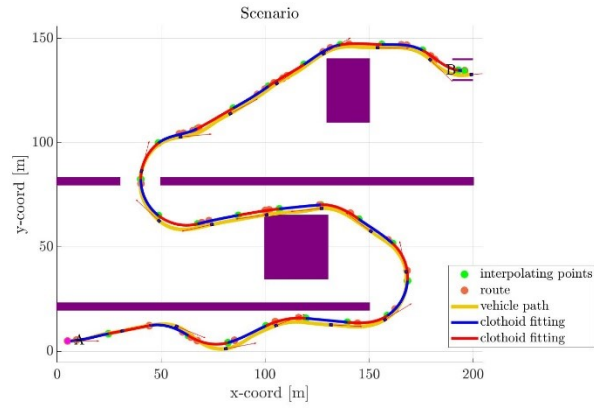


Fig. 86 Trajectory tracking with Stanley dynamic controllers at 60km/hr speed and

$$K_e, K_y = 0.1$$

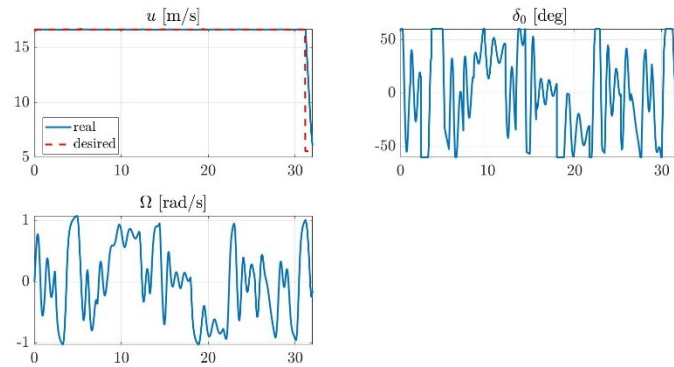


Fig. 87 Steering variation with Stanley dynamic controllers at 60km/hr speed and

$$K_e, K_y = 0.1$$